CHAPTER 9.2
LASERS

James E. Miller, Daniel S. Horowitz, Richard R. Shurtz II, Edward J. Sharp, Patrick R. Manzo, Gareth M. Janney, Bart H. Verbeek

LASER FUNDAMENTALS

James E. Miller, Daniel S. Horowitz

Laser Light Versus Nonlaser Light

The main characteristic of laser light is coherence, although laser light is usually more intense, more monochromatic, and more highly collimated than light from other sources.

Coherence is the property wherein corresponding points on the wavefront are in phase. A coherent beam can be visualized as an ideal wave whose spatial and time properties are clearly defined and predictable. Ordinary noncoherent light consists of random and discontinuous phases of varying amplitudes. The noncoherent beam has an average intensity and a predominant wavelength, but it is basically a superposition of different waves. The characteristic grainy appearance of laser light is a result of interference effects that result from coherence.

Intensity of laser light can be very high. For example, power densities of over 1000 MW/cm^2 can be obtained. A beam of such intensity can cut through and vaporize materials.

A laser beam is often highly *monochromatic* and highly *collimated*, both varying with the type of laser.

Stimulated Versus Spontaneous Emission

The laser operates on the principle of stimulated emission, an effect which is rarely observed except in connection with lasers.

Spontaneous Emission. This is the usual method whereby light is emitted from excited atoms or molecules. Assume that the laser material has energy levels, which can be occupied by electrons, that the lowest level or ground state is occupied, and that the next upper level is unoccupied. An excitation process can then raise an electron from the ground state to this upper state. The electron, after a variable time interval, returns to the ground state and emits a photon whose direction and phase of the associated wave are random and whose energy corresponds to the energy difference between the states. The upper-level lifetime may be comparatively short (less than 10 ps) or it may be long (greater than 1 μs), in which case the level is referred to as *metastable* and the light emission is *fluorescence*.

Stimulated Emission. When the electron is in the upper level, if a light wave of precisely the wavelength corresponding to the energy difference strikes the electron in the excited state, the light stimulates the electron to transfer down to the lower level and emit a photon. This photon is emitted precisely in the same direction,

and its associated wave is in the same phase as that of the incident photon. Thus a travelling wave of the proper frequency is produced, passing through the excited material and growing in amplitude as it stimulates emission.

Pumping and Population Inversion

The process of exciting the laser material (raising electrons to excited states) is referred to as *pumping*. Pumping can be done optically using a lamp of some kind, by an electric discharge, a chemical reaction, or in the case of the semiconductor laser, by injecting electrons into an upper energy level by means of an electric current.

A *population inversion* is necessary to initiate and sustain laser action. Normally, the ground state is almost entirely occupied and the upper level or levels, assuming they are more than a few tenths of an electron volt above the ground state at room temperature, are essentially unoccupied. When the upper level has a greater electron population than the lower level, a population inversion is said to exist. This inverted population can support lasing, since a traveling wave of the proper frequency can stimulate downward transitions and the associated energy can be amplified.

Optical Resonators

The addition of a positive-feedback mechanism to a lasing medium permits it to serve as an oscillator.

The Fabry-Perot Resonator. The Fabry-Perot resonator that provides optical feedback consists of two parallel mirrors, the rear mirror fully reflecting and the front mirror partly reflecting and partly transmitting at the laser wavelength. The light reflected back from the front and rear mirrors serves as positive feedback to sustain oscillation, and the light transmitted through the front mirror serves as the laser output. Laser action is started by spontaneously emitted light with the proper direction to travel down the axis of the laser rod and be reflected on itself from the end mirrors. The two mirrors form an optical cavity which can be tuned by varying the spacing of the mirrors. The laser can operate only at wavelengths for which a standing-wave pattern can be set up in the cavity, i.e., for which the length of the cavity is an integral number of half wavelengths. Mirrors may be separate from the laser rod or deposited on its end faces.

Spectral Modes. Spectral modes, i.e., a multiplicity of radiation patterns, are permitted within the cavity. Longitudinal modes, determined by the spacing of the mirrors, occur at each wavelength for which a standing-wave pattern can be set up in the cavity. Transverse modes vary not only in wavelength but also in field strength in the plane perpendicular to the cavity axis. The longitudinal, or axial, mode structure determines the spectral characteristics of the laser, i.e., the coherence length and spectral bandwidth, while the transverse-mode structure determines the spatial characteristics, e.g., beam divergence and beam energy distribution.

If no attempt is made to control the mode of the laser, many longitudinal modes will be seen in the output. These modes lie within the natural spectral line width of the laser transition (Fig. 9.2.1). The transverse modes depend on the physical geometry of the cavity and are denoted similarly to waveguide modes at microwave frequencies. The lowest-order mode, characterized by a narrow, diffraction-limited beam spread, is the transverse electromagnetic (TEM_{00}) mode. Higher-order modes have multilobe intensity patterns and wider beams.

Mode control, or selection, is achieved by a variety of methods, e.g., varying the mirror curvatures, restricting the beam by apertures in the cavity, using resonant reflectors that reflect only a narrow band of wavelengths, and using Q-switching techniques.

Generation of Laser Pulses

The typical output of an optical laser consists of a series of spikes occurring during the major portion of the time the laser is pumped (Fig. 9.2.2). These spikes result because the inverted population is being alternately built up and depleted. *Q switching* (Q spoiling) is a means of obtaining all the energy in a single spike of very high peak power. As an example, an ordinary laser might generate 100 mJ over a time interval of 100 μs for a peak power (averaged over this time interval) of 1000 W. The same laser Q-switched might emit 80 mJ in a single 10-ns pulse for a peak power of 8 MW. The term Q switching is used by analogy to the Q of an electric circuit. Lowering the Q of the optical cavity means the laser cannot oscillate, and a large inverted population builds up.

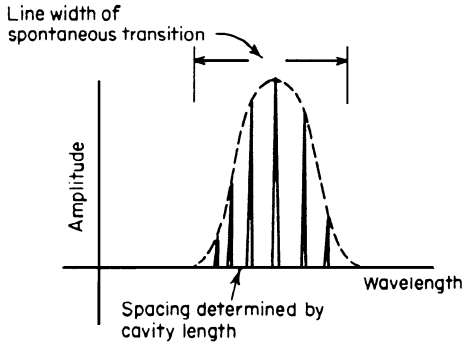

FIGURE 9.2.1 Typical spectral modes of an optically pumped laser.

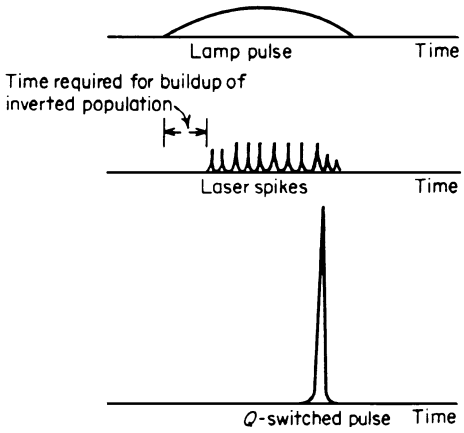

FIGURE 9.2.2 Typical output of an optically pumped laser for *Q*-switched and non-*Q*-switched operation.

When the cavity *Q* is restored, a single "giant pulse" (see Fig. 9.2.2) is generated. This high-peak-power pulse is useful in optical ranging and communication and in producing nonlinear effects in materials.

Q switches use five techniques to inhibit laser action: the mechanical, or movable-optical-element, *Q* switch; the saturable organic-dye absorber; the electro-optic-effect crystal; the magneto-optic-effect crystal; and the acousto-optic-effect crystal.

All *Q* switches except the saturable absorber operate by deflecting radiation out of the optical cavity to prevent laser oscillation. The saturable absorber, called a *passive Q* switch because no external signal is required, consists of an organic compound usually in a liquid solution placed between the laser medium and one of the cavity mirrors. The dye is initially very highly absorbing at the laser wavelength, and the laser is isolated from one mirror. The absorbing transition in the dye is saturated as its ground state is depopulated, causing the dye to become transparent, or "bleach." The rate of bleaching is a strongly nonlinear function of incident radiation, and as the population inversion increases, the dye rapidly switches to a highly transparent state to allow lasing to occur.

Mode locking (phase locking). This technique leads to even shorter pulses. A free-running laser output consists of a time average of many longitudinal and transverse modes with no fixed phase and amplitude relationship. If the laser is constrained to oscillate in only one transverse mode, there are still many longitudinal modes spaced in frequency at intervals of $c/2L$ (L = cavity length), which contribute randomly to the output. The time dependence of the output will be controlled by constraining these modes to maintain a fixed phase and amplitude relationship. A narrow pulse in the time domain requires a wide bandwidth in the frequency domain. The output of a mode-locked laser is a series of pulses, approximately $1/\Delta\nu$ wide, where $\Delta\nu$ is the laser gain bandwidth. These pulses are spaced at intervals of the cavity round-trip transit time.

Frequency Selection

Methods of frequency (or wavelength) selection vary with the type of laser. The following techniques are typical. For solid-state lasers, the output frequencies are limited to a few sharp closely spaced lines. The wavelength of these lines depends on the active ion in the laser, and the specific wavelength is chosen by a highly selective dielectric mirror or a dispersive prism used as part of the optical cavity. Liquid lasers have broad emission bands, several tens of nanometers wide. The output wavelength can be continuously tuned within this band by an intracavity prism or diffraction grating.

Semiconductor lasers have narrow emission bands determined by the constituents. For a given semiconductor, the output wavelength can be varied by changing the temperature. Gas lasers emit discrete lines at wavelengths depending on the gas. Specific lines are chosen by a diffraction grating or prism. Some gas lasers are pumped by a second gas laser. The wavelength of this type of laser is controlled by the wavelength of the pump laser as well as the cavity elements described previously.

CLASSES OF LASERS AND THEIR BASIC APPLICATIONS

Richard R. Shurtz II

Primary Characteristics of the Laser Classes

Lasers can be divided into the four basic categories shown in Table 9.2.1: gas, solid-state optically pumped, liquid dye, and semiconductor. Combined, these lasers cover the spectral region from ultraviolet (0.1 μm) to far infrared (1000 μm), available wavelengths most densely populating the visible to infrared region.

The rapid development of new lasers over the past several years has created a dynamic and continually changing ensemble of devices available to the applications engineer. This set has stabilized as the most useful lasing systems have become known commodities and commercially available. In this section we quantify this established set of commercial devices and outline the primary applications base of each laser type. The reader should be able to identify the laser system best suited for a particular application and then refer to the appropriate paragraph for more specific information.

Gas lasers, shown in the top bar of Table 9.2.1, have the broadest spectral coverage.

The solid-state optically pumped laser category spans the visible to near infrared region. This is the only laser class that can be *Q*-switched or cavity-dumped. The electronic transitions are pumped either by flash lamps or by semiconductor diodes.

The family of *optically pumped organic-dye lasers* extends in wavelength from 0.4 to 1 μm. The major distinction of the category is its continuous tunability over the entire visible spectrum. Because of their

TABLE 9.2.1 Four Classes of Lasers

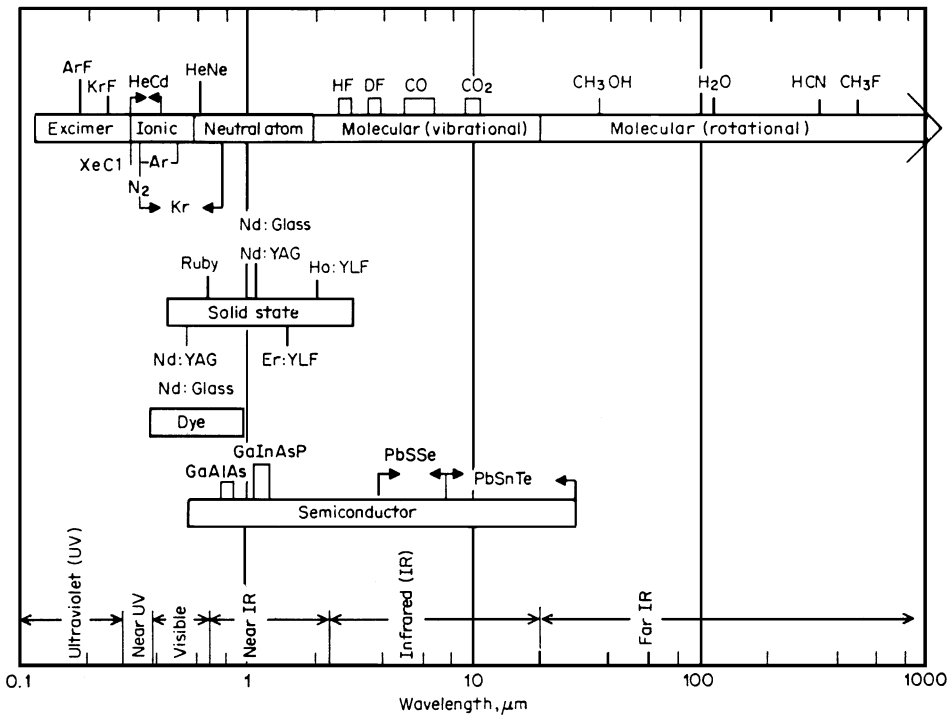

TABLE 9.2.2 Properties of Commercially Available Pulsed Lasers

Laser	Type	Wavelength, μm	Output, J		Pulse per second	Pulse length, μs	Beam diam, mm	Beam divergence, mrad
			TEM_{00}	Multimode				
XeCl	Excimer	0.308	. . . . .	0.015–80	1–90	0.005–0.01	6 × 18–10 × 25	4–2 × 5
Nitrogen	Molecular gas	0.337–0.427	400–800 kw	0.002–0.01	1–100	0.005–0.01	6 × 20–10 × 25	1 × 7–5 × 10
Dye	Organic solution	0.39–1	. . . . .	10^2–10^6 W	1–10^3	10^{5}–^{5}–0.8		
Ruby	Solid state	0.694	0.02–5	0.3–50	0.1–1	10^{-5}–10^4	1.5–20	0.4–8
GaAlAs	Semi-conductor	0.8–0.9	. . . . .	0.1–3000 W	1–10^4	5 × 10^2–1	. . . . .	100–300
Nd:Yag	Solid state	1.06	5 ×10^{-3}–5	0.1–400	1–100	10^{-5}–10^4	1.5–75	0.3–12
Nd:Glass	Solid state	1.06	10^3–60	0.3–10^3	0.02–5	10^{-5}–10^4	2–120	0.1–10
Ho:YLF	Solid state	2.06	. . . . .	0.001–0.01	10–10^3	0.07–100	3	5
CO_2	Molecular gas	9–11	0.01–10^4	0.2–10^4	1–10^4	0.1–10^7	1–350	0.3–10
HCN	Molecular gas	337	0.001	. . . . .	1–100	30	10	40

broadband spectral output, these lasers can generate subpicosecond pulses when mode-locked. Their primary use is in spectroscopy and photochemistry.

Semiconductor lasers are pumped by the injection of excess electrons and holes into a thin semiconductor layer. Radiation is produced when the excess carriers recombine, producing photon energies equal to the bandgap energy. Lead salt laser diodes operate from 4 to 30 μm, continuously tunable either by varying the drive current or the temperature. They are used primarily for spectroscopy and must be cooled to nominally 77 K during operation. The shorter-wavelength semiconductor lasers are formed from III-V compounds: gallium arsenide (GaAs), gallium aluminum arsenide (GaAlAs), and gallium indium arsenide phosphide (GaInAsP). These devices, either pulsed or cw, operate at room temperature.

Single III-V compound laser diodes are used for fiber-optic communication, integrated optical processing, and rangefinding. Arrays of diodes are used for low-power infrared illuminators.

Characteristics of commercially available pulsed and cw lasers are summarized in Tables 9.2.2 and 9.2.3. The ranges shown are based on tables published in laser buyers' guides. A few key lasers have been selected to illustrate the essential properties of each laser category, as discussed in the previous paragraphs.

TABLE 9.2.3 Properties of Commercially Available Continuous Wave (cw) Lasers

Laser	Type	Wavelength, μm	Power, W		Beam diam, mm	Beam divergence, mrad
			TEM_{00}	Multimode		
Argon (Ar)	Ionized gas	0.33–0.5145	4 × 10^{-3} –18	4 × 10^{-3}–22	0.8–2	0.5–1.5
Krypton (Kr)	Ionized gas	0.33–0.799	0.5–10	0.5–6	1–2	0.6–2
He-Cd	Ionized gas	0.325–0.442	10^{-3}–4 × 10^{-2}	1.5 × 10^{-3}–6 × 10^{-2}	0.82–1.5	0.5–1.6
Dye	Organic solution	0.39–1	. . . . .	0.1–1	0.5–0.7	1.4–2
He-Ne	Neutral gas	0.6328	10^{-3}–2	10^{-2}–1.3	0.45–30	0.71–2.1
GaAlAs	Semiconductor	0.8–0.89	. . . . .	10^{-3}–10^{-2}	. . . . .	5–610
Nd:YAG	Solid state	1.06	0.2–18	0.4–100	0.8–7	1.5–15
Ho:YLF	Solid state	2.06	. . . . .	5	3	25
CO_2	Molecular gas	9–11	1–10^4	4–10^4	1–70	1–10
HCN	Molecular gas	337	0.01–1	. . . . .	10	40

TABLE 9.2.4 Selected Laser Applications

Application	Technique	Mode of operation*	Desired laser property	Possible laser
Measurement				
Distance, short range	Interferometric	cw	Coherence	He-Ne
Long range	Time of flight	P	Short pulse length	Q-switch Nd:YAG, GaAS
Shape, thickness	Refraction measurement	cw	Collimation, transparency	He-Ne
Diameter	Interference	cw	Coherence	He-Ne
Overall dimension	Obscuration	cw	Collimation	He-Ne
Imperfections	Interference, obscuration	cw	Coherence, collimation	He-Ne or other cw for transparency
Alignment	Beam used as reference	cw	Collimation, visibility	He-Ne
Atmospheric monitoring				
Wind, turbulence	Doppler-shifted particulate backscatter	P†	Short pulse, narrow, bandwidth	CO_2, Nd:YAG
Particulate	Backscatter	P	Short pulse	CO_2, Nd_1:YAG
Gaseous pollution	Raman-shifted backscatter	P	Short pulse, narrow band width	CO_2, Nd_1:YAG
	Absorption	cw	Tunable, narrow bandwidth	PbSnTe diode, dye
	Fluorescence	cw	Tunable, narrow bandwidth	PbSnTe diode, dye
Material removal				
Drilling	Energy concentration	P	1–10 MW/cm^2	Ruby, Nd:YAG, Nd:glass
Cutting	Energy concentration	P, cw	1–10 MW/cm^2	CO_2, Nd:YAG
Film vaporization	Energy concentration	P, cw	100 kW/cm^2	CO_2, Nd:YAG, argon, xenon
Scribing wafers	Energy concentration	P, cw	100 kW/cm^2	CO_2 Nd:YAG
Illumination (infrared)	Pulse-gated for particulate penetration	P	Narrow pulse, efficient	GaAlAs diodearrays
Heating				
Welding	Energy concentration	P, cw	1–10 MW/cm^2	Nd:YAG, CO_2
Heat treating, annealing	Energy concentration	P, cw	Moderate to high power	Nd:YAG,CO_2, ruby
Fusion	Energy concentration	P	100 TW per 50-μm particle	Nd:glass, CO_2
Communications				
Fiber optic	Digital; analog	P, cw	Bandwidth; linear output	cw GaAlAs; cw GaInAsP
Space	Analog	cw	Stability collimation	CO_2
Optical information				
Processing	Integrated optics; three-dimensional optics	cw	Coherence	cw GaAlAs; coherent cw gas

TABLE 9.2.4 Selected Laser Applications (*Continued*)

Application	Technique	Mode of operation*	Desired laser property	Possible laser
Storage	Holography	cw	Coherence	He-Ne, argon
Chemical				
Laser-induced reactions	Selective breaking of bonds	P, cw	Tuning to molecular resonance	Variety of moderate-power lasers
Spectroscopy	Absorption; Raman emission	cw	Narrow bandwidth, tunable	Organic dye, PbSn Te diode
Isotope separation, e.g., uranium	Chemical isolation of excited species	cw	Laser tuned to excite one species	Organic dye, PbSn Te diode, others
Medical				
Skin treatment	Laser-induced reactions	P, cw	Tuned to resonant absorption	Ruby, tunable dyes, ultraviolet lasers
Surgery	Cutting, cauterization	P, cw	Collimation, power	Nd:YAG, CO_2, argon
Eye repair	Retina repair	P, cw	Collimation, power	Ruby, argon
Destructive weapons	Energy concentration	P, cw	High average power	CO_2, HF

*cw = continuous wave, P = pulsed.
†For range.

Laser Applications

Laser applications can be divided into several general categories: measurement of spatial parameters, material heating and/or removal, nondestructive probing of resonant phenomena, communications, optical processing, laser-induced chemical reactions, and weapons. Selected laser applications are shown in Table 9.2.4.

SOLID OPTICALLY PUMPED LASERS

Edward J. Sharp

Basic Principles

A solid optically pumped ionic laser consists of a solid material with optical gain, situated inside a resonator formed by two or more mirrors. Spontaneous emission in the material is amplified by stimulated emission. The resonator provides the feedback for the optical amplifier, resulting in a laser oscillator. The optical arrangement for a typical optically pumped laser is shown in Fig. 9.2.3.

These devices generally consist of a pump reflector enclosing the laser rod and optical pump in one of the number of efficient ways which is usually determined by the application or laser property to be exploited. The laser rod is pumped by flash lamp for pulsed operation and usually by arc lamps for cw (continuous-wave) operation, or in some cases an appropriate laser can be selected for the optical pump.

Two important conditions must be met: the wavelength region of the pump emission must overlap a significant portion of the absorption spectrum of the active ion or ions which are incorporated in the laser rod, and the optical pump must not damage the laser rod. Figure 9.2.4 illustrates the overlap of pump emissions and the absorption bands of a typical Nd^{3+} four-level laser scheme where pumping is accomplished by xenon-lamp pumping and LED laser pumping.

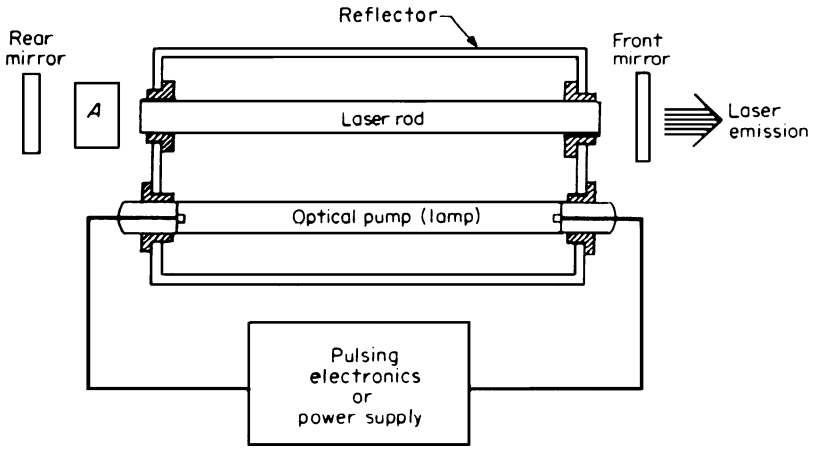

FIGURE 9.2.3 Typical optically pumped laser configuration. Component *A* can represent a *Q* switch, polarizer, or other optical element.

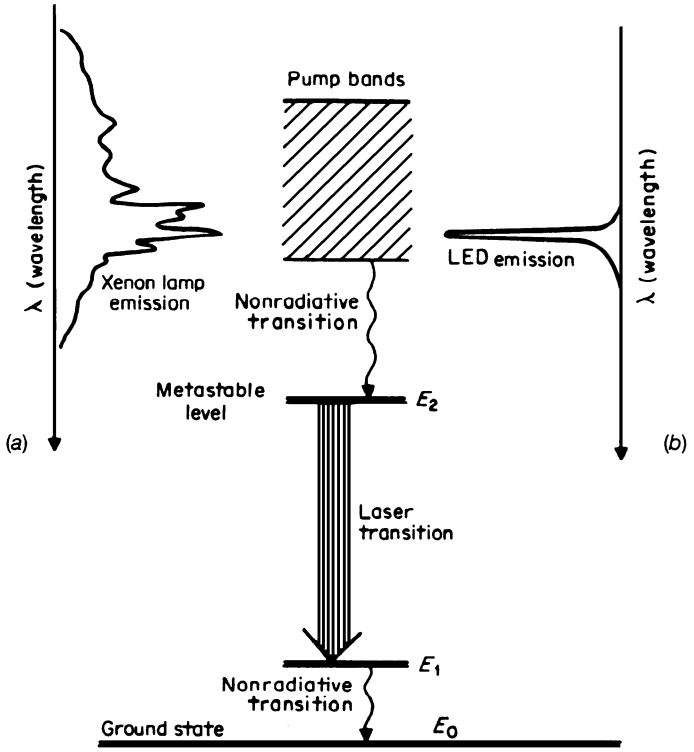

FIGURE 9.2.4 A typical four-level Nd^{3+} laser, in which the Nd^{3+} ions are optically excited by pumping the absorption bands of the ions with (*a*) a xenon lamp and (*b*) an LED laser.

Laser Components

Optical Pumps. The general technique of optical pumping has many uses. To achieve population inversion linear, low-pressure flash lamps are the most common pumping device. Typically they have tungsten electrodes and are filled to a few atmospheres pressure with xenon or krypton. For pulsed operation xenon is commonly used but the lines of krypton radiate at wavelengths more favorable than xenon for pumping a neodymium laser at low input levels. Thus it is a more efficient cw pump. At higher input levels, the blackbody spectrum becomes stronger than the emission lines, and this advantage is lost.

Pulsing Electronics. For pulsed operation the energy to be discharged into a flash lamp is stored in a capacitor and discharged through the lamp via a choke whose value is selected to give the desired pulse width with minimum ringing. The spectrum of the lamp discharge depends on the electrical parameters, pressure, and fill gases, so that it can be tailored to match the absorption bands of the active ion to a certain extent.

Coolants. Lasers that operate cw or at a high repetition rate need to be cooled, since most of the energy expended in the flash lamp is converted into heat and would quickly cause overheating and/or thermal cracking of the laser rod. Air and liquids have been successfully used as coolants, liquids being used when cooling requirements are more severe. Distilled or deionized water is often used, and mixtures of water and ethylene glycol are used for operation below 0°C. The coolant circuit includes a pump for circulation and a radiator, often with a fan, to dissipate the heat.

Pumping Reflectors. To obtain maximum use of the pump light, it must be efficiently collected and coupled into the rod. The reflectors used to do this are usually elliptical in cross section, with a rod at one focus and the lamp at the other. Sometimes two lamps are used, in a double elliptical cavity. Often a round cross section is used, resulting in an afocal system. In general, the smallest cross section is best, and the highest efficiency is obtained with a close-coupled arrangement, where the rod and lamp are almost in contact and the reflector encloses them closely. However, in this close-coupled configuration the thermal distortion of the rod owing to the asymmetrical pumping could be a serious problem.

Mirrors. Multilayer dielectric mirrors can be deposited on the laser-rod ends, which are finished flat and parallel. These mirrors are designed for specific reflectivities at the operating wavelengths and eliminate the problem of alignment. The rear-mirror reflectivity is normally 100 percent, but the front-mirror reflectivity is selected for the best performance, determined by laser-material properties, rod size, and operating power level. Where separate mirrors are used (see Fig. 9.2.3) the rod ends should be antireflection-coated or cut at Brewster's angle. Separate or external mirrors must be mounted in holders that permit fine adjustment about two axes to achieve the required parallelism.

Q-Switched Lasers

Q switching, a technique used for generating large output bursts of radiation from laser devices, is accomplished by effectively blocking the optical path to one of the mirrors for most of the time during which the rod is being pumped, causing the rod to store energy. The *Q* switch then quickly restores the optical path to the mirror and a giant pulse (see Fig. 9.2.2) is generated. The four main types of *Q* switches are the rotating mirror, acousto-optical, electro-optical, and saturable absorber.

Rotating Sector, Prism, or Mirror. The rotating prism or mirror requires careful mechanical design to provide rotation at the required speeds (30,000 r/min is common) and still maintain alignment. They are generally less reliable than other methods of *Q* switching, but the extinction ratio is infinite and the insertion loss is negligible, enabling this type of *Q* switch to attain high efficiencies.

Electro-Optic Q Switches. An electro-optical crystal, or liquid Kerr cell, can be placed in the optical resonator, usually between the rear mirror and the laser rod (position *A* in Fig. 9.2.3) along with an appropriate

polarizer to effect the cavity losses. The polarization of the light passing through the electro-optic medium is changed by the application of an applied electric field and is rejected by the polarizer. When the voltage is removed, the cavity losses are reduced, permitting giant-pulse radiation.

Acousto-optic Q switch. An acousto-optic Bragg scattering switch deflects the beam, which is then used to provide feedback during the buildup time. In these devices a standing-wave pattern of ultrasonic waves is set up in a suitable cell positioned in the resonator. The refraction resulting from the passage of a plane-parallel light beam through this ultrasonic field is sufficient to provide shuttering action for infrared lasers, leading to giant-pulse radiation.

Saturable absorber Q switch. These switches are usually bleachable dyes that undergo decreased absorption at high light intensities. They are known as passive *Q* switches since they do not require any electrical or mechanical control. The material is opaque until the fluorescence of the laser rod bleaches it and the optical path is restored for a *Q*-switched pulse.

Ions and Hosts

The current list of ions which can be incorporated into a solid host and made to lase numbers about 20. The total number of different wavelengths available from these ions is approximately 150. The solid host is any crystal or glass that can accommodate trivalent or divalent rare-earth and iron-group ions. The iron-group ions in which laser oscillation has been achieved are divalent nickel and cobalt and trivalent chromium and vanadium. The rare-earth ions in which laser oscillation has been achieved are divalent samarium and dysprosium and trivalent europium, praseodymium, ytterbium, neodymium, erbium, thulium, and uranium.

Characteristics of the Hosts

The host material to which the active ion (dopant) is incorporated can be either crystalline or glass and should exhibit the following properties:

- High thermal conductivity
- Ease of fabrication
- Hardness (to prevent degradation of optical finishes)
- Resistance to solarization or radiation-induced color centers
- Chemical inertness, i.e., not water soluble
- High optical quality, which implies uniformity of refractive index and absence of voids, inclusions, or other scattering centers

Crystalline Hosts. Crystalline hosts offer as advantages in most cases their hardness, high thermal conductivity, narrow fluorescence line width, and, for some applications, optical anisotropy. Crystalline hosts usually have as disadvantages their poor optical quality, inhomogeneity of doping, and generally narrower absorption lines.

Glass Laser Hosts. Glass laser hosts are optically isotropic and easy to fabricate, possess excellent optical quality, and are hard enough to accept and retain optical finishes. In most cases glasses can be more heavily and more homogeneously doped than crystals, and, in general, glasses have broader absorption bands and exhibit longer fluorescent decay times. The primary disadvantages of glass are its broad fluorescence line widths (leading to higher thresholds), its significantly lower thermal conductivity (a factor of 10 leading to thermally induced birefringence and distortion when operated at high pulse-repetition rates or high average powers), and its susceptibility to solarization (darkening because of color centers that are formed in the glass as a result of the ultraviolet radiation from the flash lamps). These disadvantages limit the use of glass laser rods for cw and high-repetition-rate lasers.

Sensitized Lasers

Laser performance and efficiency can be enhanced through the technique of energy transfer. A second ion (sensitizer) is incorporated into the host in addition to the laser ion (activator) to accomplish this effect. The sensitizer may be a color center. Pump energy is absorbed by the sensitizer and is transferred to the activator, which then emits this energy at the laser wave-length.

Miniature Lasers

Several host materials that incorporate Nd as a constituent rather than a dopant, such as $NdAl_3(BO_3)_4$, neodymium aluminum borate (NAB); $LiNdP_4O_{12}$, lithium neodymium tetraphosphate (LNP); and NdP_5O_{14}, neodymium pentaphosphate (NdPP), have been studied recently, and since concentration quenching is not appreciable in these materials, they are excellent candidates for miniaturized lasers.

LIQUID LASERS

Patrick R. Manzo

Laser Media

Liquid Lasers. Liquid lasers use a liquid as the laser medium in place of a large single crystal or a gas (Fig. 9.2.5). Their properties are intermediate between those of gaseous and solid lasers. They are easy to prepare in large samples with excellent optical quality, and for certain types their energy output can be as high as 10^8 W peak and several tens of watts average. The wavelength coverage available for certain types of liquid lasers is considerably greater than that of both the solid and the gaseous lasers. There are two types of liquid lasers in common use.

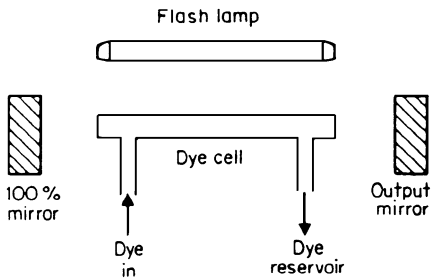

FIGURE 9.2.5 Typical dye-laser configuration.

The aprotic liquid laser consists of a rare-earth salt dissolved in an inorganic solvent that does not contain hydrogen. Energy from the excitation source is absorbed by the solvent and then transferred to the rare-earth ion, which lases. The absence of hydrogen in solution greatly increases the efficiency of this energy-transfer process because it lessens the possibility of this energy being transferred into vibrations of the molecule. The output wave-length is that of the rare-earth salt (see Table 9.2.1). In system gain, in output power levels, and in overall efficiencies, the aprotic liquid lasers are comparable with the solid-state lasers. They are capable of extremely high peak powers (10^8 W) and sustained high average powers (50 to 100 W). The principal aprotic liquid laser materials are Nd^{3+} in $SeOCl_3$ with $SnCl_4$ or in $POCl_3$ with $SnCl_4$.

The *dye laser* uses highly fluorescent organic molecules as the laser medium; unlike the aprotic liquid, these molecules do not contain the rare-earth salts. The radiative transition in the dye laser does not originate at a metastable energy level, as in most other lasers, but takes place instead between two singlet electronic states of the molecule. Consequently it is strongly allowed and extremely short-lived—approximately 10 ns compared with several hundreds of microseconds for the rare-earth ions. This requires quite different excitation techniques to achieve laser action. The first organic dye lasers required *Q*-switched lasers or flash lamps with extremely fast rise times in order to invert the population fast enough to achieve laser action. However, newer techniques alleviate the necessity for such fast excitation sources. Rhodamine 6G and several other dyes have been made to operate in a continuous mode with average power as high as 10 W.

The organic dyes exhibit excellent optical quality in solution, and they are extremely easy to prepare and handle. The absorption and fluorescent bands of the molecule are extremely broad (several tens of nanometers) because of the large number of vibrational and rotational energy levels associated with each electronic energy level. The laser output can be broadband (30 nm wide) or very narrow (0.001 nm).

The very short lifetime of the excited state means that sources must be of very high intensity to cause the dyes to lase. Therefore, the sources used to pump the dyes include high-intensity flash lamps and other lasers. Distortion in the dye because of thermal inhomogeneities requires that the dye be mixed rapidly and exchanged in order to minimize beam spreading and losses during cw and repetition-rate operation. The line width of typical dye materials is homogeneously broadened, and therefore all the stored energy in the upper laser level can be channeled into a spectrally narrow emission line, which can be tuned over the gain profile of the active medium.

Flashlamp-pumped dye lasers have demonstrated average powers as high as 100 W at high repetition rates. Single pulse energies to 10 J per pulse and peak powers to 10 MW have also been demonstrated. Present flashlamp-pumped systems are limited to approximately 1 percent efficiency while the efficiency of laser-pumped dyes is somewhat lower. Average power from a few milliwatts to over 10 W has been achieved in cw operation of laser dyes using pump laser configurations such as the one shown in Fig. 9.2.6*a*. Frequency-stabilized cw dyes have achieved a line width of less than 1 MHz and long-term stabilities of a few hundred hertz.

With an appropriate selection of dyes, this type of laser can be directly tuned from 340 to 1200 nm. This wavelength range has been extended into the ultraviolet and the infrared by frequency mixing of dye-laser radiation in nonlinear optical materials. Tunable ultraviolet radiation down to 196 nm has been obtained by second-harmonic and sum-frequency generation in nonlinear crystals. In the long-wavelength range the generation of tunable near and middle infrared, as the difference frequency of two laser oscillators, has been successful out to 12.7 μm. It is also possible to produce multiple wavelengths from the same or combination of dyes. Figure 9.2.6*b* illustrate one scheme for doing so.

It is possible to produce dye laser pulses with a duration of less than 1 ps. Durations as short as 0.3 ps have been reported. In addition, the broad emission bands of dyes make them the only sources capable of producing mode-locked picosecond pulses at high repetition rates which are wavelength tunable over several tens of nanometers.

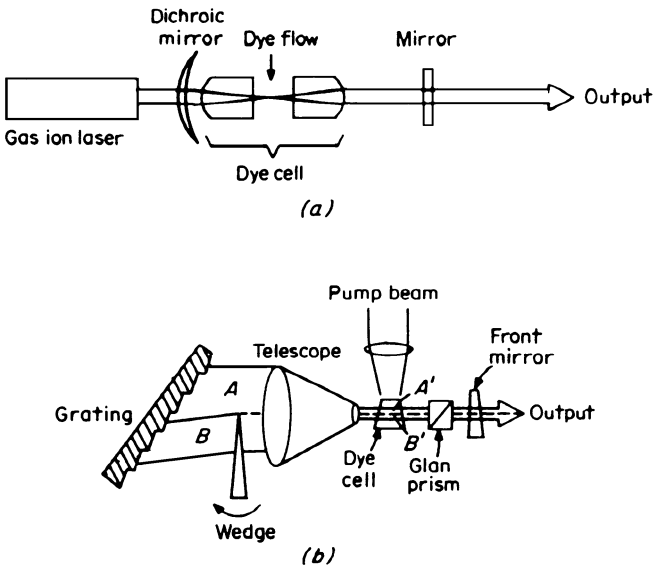

FIGURE 9.2.6 (*a*) Schematic of a continuous-wave dye laser; (*b*) double-wavelength dye laser. The lower portion of the beam is shifted toward the red by the wedge.

GAS LASERS

Gareth M. Janney

General Characteristics

Gas lasers can best be characterized by their variety. The laser medium may be a very pure, single-component gas or mixture of gases. If may be a permanent gas or a vaporized solid or liquid. The active species in a gas laser may be a neutral atom, an ionized atom, or a molecule (including excimers, which are "stable" molecules only in an excited state). The operating pressures range from a fraction of a torr to atmospheric pressure, and the operating temperature from –196 to 1600°C. Excitation methods include electric discharges (glow, arc, pulsed, rf, dc), chemical reactions, supersonic expansion of heated gases (gas dynamic), and optical pumping. The average output power of useful gas lasers range from a few microwatts to tens of kilowatts (10 orders of magnitude), and the peak power ranges from a fraction of a watt to 100 MW. The range of output wavelengths extends from 0.16 to 744 μm at discrete wavelengths.

Multiple Wavelengths

Most gas laser materials have a number of distinct laser transitions (i.e, different wavelengths). For example, the neon atom has more than 100, and the argon ion has more than 30. Lasers using these materials can operate with a multiwavelength output, or one transition at a time can be selected by a simple adjustment (rotating a prism or diffraction grating in the optical cavity). Table 9.2.5 (bottom) shows several commercially available lasers that provide more than one wavelength of operation.

Electrically Excited Electric-Discharge Gas Lasers

Most gas lasers are excited by electric discharges. Electrons that have been accelerated by an electric field transfer energy to the gas atoms and molecules by collisions. These collisions may excite the upper laser level directly. Indirect excitation is also possible by cascading from higher-energy levels of the same atom (or molecule) or resonant-energy transfer from one atom (or molecule) to another by collision.

Typical configuration (Fig 9.2.7). The gas is contained in a glass tube having an electrode near either end. The ends are sealed by windows mounted at Brewster's angle to minimize reflections at the windows (for one plane of polarization). An optical cavity is formed by two mirrors (usually both are concave), at least one of which is partially transmitting. When an electric discharge is produced in the tube between the electrodes, the gas atoms or molecules are excited and laser action starts. Listed below are some typical parameters for several common types of electric-discharge gas lasers.

Laser species	Gas mixture	Pressure, torr	Current, density A/cm^2
Ne (neutral atom)	He	1.0	0.05–0.5
	Ne	0.1	
Ar (ion)	Ar	0.3	100–2000
CO_2	He	5–10	0.01–0.1
	N_2	1.5	
	CO_2	1.0	

The Transverse-Electric-Discharge Configuration (Fig. 9.2.8). The transverse-electric-discharge configuration is used for some gas lasers, especially for high-average-power, fast-flowing gas lasers. It provides high electric fields at practical voltages while retaining long paths of excited gas.

TABLE 9.2.5 Representative Gas Lasers*

Continuous-wave (cw)				
		Power, W		
λ, μm	Laser type	Typical	Max	Comment
0.3252	HeCd	10^{-3}–10^{-2}		Metal vapor, electric discharge
0.33–0.53	Ar	0.5–5	20	High-current electric discharge
0.33–1.09	Ar/Kr	0.5	6	High-current electric discharge
0.4416	HeCd	$1–5 \times 10^{-3}$		Metal vapor electric discharge
0.46–0.65	HeSe	10^{-3}		Metal vapor electric discharge
0.6328	HeNe	10^{-3}	10^{-1}	Most common gas laser
1.15	HeNe	10^{-3}		
1.315	I_2		10^2	Experimental chemical laser
2.6–3.0	HF	5–50	10^4	Chemical laser
3.39	HeNe	10^{-3}	10^{-2}	
3.5	HeXe	5×10^{-3}		
3.6–4.0	DF	2–100	10^4	Chemical laser
5–6.5	CO	2–10	50	
9–11	CO_2	1–100	10^4	Optically pumped by CO_2 or CO laser
27–374	H_2O	$1–10 \times 10^{-3}$		
34–388	NH_3	10^{-3}		
311, 337	HCN	10^{-2}	1.0	
37–1217	Methanol	$1–10 \times 10^{-4}$		

Pulsed lasers				
		Pulse energy, J		
λ, μm	Laser type	Typical	Max	Comment
0.157	F_2	10^{-2}		
0.193	ArF	10^{-1}		
0.222	KrCl	10^{-2}		
0.248	KrF	10^{-1}	10^2	*e* beam for high energy
0.308	XeU	10^{-1}		
0.337	N_2	10^{-3}–10^{-2}		
0.351	XeF	10^{-1}		
0.458–0.53	Ar	10^{-8}–10^{-6}		
0.5105, 0.5782	Cu	10^{-4}–10^{-3}		
1.5	Ba	10^{-3}		
2.8–3	HF	1	2×10^2	Chemical, electrically initiated
3.6–4.1	DF	10^{-1}–1		Chemical, electrically initiated
9–11	CO_2	10^{-1}–10^2	10^4	*e* beam for high energy
118.8	Methanol	10^{-3}		
496.1	Methyl fluoride	10^{-4}		

Multiple-wavelength gas lasers				
Laser type	Wavelength, μm			Comment
Helium-neon	0.5939	0.6352	1.152	Rotate prism to select one wavelength at a time
	0.6046	0.6401	1.162	
	0.6118	0.7305	1.177	
	0.6294	1.080	1.199	
	0.6328	1.084	3.39	

TABLE 9.2.5 Representative Gas Lasers* (*Continued*)

Multiple-wavelength gas lasers				
Laser type	Wavelength, μm			Comment
	Argon	Krypton	Xenon	
Noble-gas ions	0.3511	0.4619	0.4955	Rotate prism to select lines from one gas; change gas in tube to change set of wave lengths, mixtures of gases can be to extend range; simultaneous oscillation on many lines possible
	0.3638	0.4762	0.5007	
	0.3795	0.5208	0.5160	
	0.4579	0.5682	0.5260	
	0.4965	0.6471	0.5353	
	0.5017	0.6764	0.5395	
	0.5145		0.5959	
	0.5287			
Carbon dioxide		9.1–11.3		Several groups of closely spaced lines in this wavelength region; line separations within groups ~0.02 μm; rotate diffraction grating to select lines one at a time

*Wavelength ranges are sets of discrete wavelengths and simultaneous output at more than one wavelength may or may not be possible.

A pair of long electrodes (or linear arrays of electrodes) is located parallel to the optical axis, within the envelope that contains the gas. The discharge current flows transverse to the optical axis. Lasers employing this configuration include high peak power, pulsed N_2, Ne, and CO_2; high-average-power, fast-flowing CO_2 lasers; and excimer lasers (e.g., XeF, KrF).

E-Beam Lasers. High-energy high-current electron beams are generated in an evacuated high-voltage electron gun. The electron beam passes through a thin metal foil into a chamber containing the gas mixture. As in electric-discharge lasers, some of the kinetic energy of the electrons is transferred directly or indirectly to the laser species (atom or molecule). Electron beams are sometimes used in conjunction with transverse electric discharges.

Chemical Lasers

Chemical lasers derive their energy from the free-energy change of a chemical reaction. The chemical reaction may be initiated by some other source of energy, such as light or electric discharges. Since the chemical reaction consumes the reactants, a flowing system is necessary for repetitive-pulsed or cw operation. Figure 9.2.9 shows an arrangement used to produce high-power, cw laser output from hydrogen fluoride (HF) and other

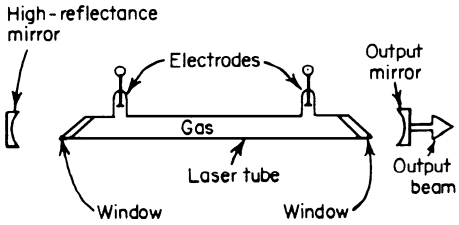

FIGURE 9.2.7 Electric-discharge gas laser.

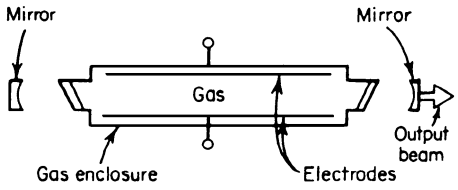

FIGURE 9.2.8 Transverse-electric-discharge gas laser.

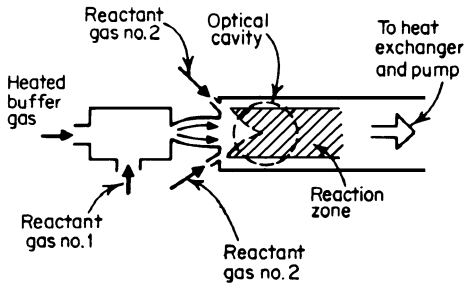

FIGURE 9.2.9 Fast-flowing chemical laser.

molecules. A series of chemical reactions is required to sustain the laser operation in practice, but in simplified form the reaction can be expressed as

$$F_2 + H_2 \rightarrow 2HF + \Delta E$$

where F_2 = reactant, 1
H_2 = reactant 2
ΔE = free-energy change, some of which is in the form of vibrationally excited HF molecules

Laser action occurs on vibrational transitions of the HF molecule in the wavelength region 2.6 to 2.9 μm. Chemical lasers of this general type are potential sources of high average power (multikilowatt).

Gas Dynamic Lasers

The expansion of a hot, high-pressure mixture of CO_2 and N_2 through a supersonic nozzle results in a lowering of the gas temperature in a time which is short compared with the vibrational relaxation time of the CO_2 molecule. A differential relaxation time between the upper and lower laser levels results in a population inversion for a short distance downstream from the supersonic nozzle, and laser operation in this region is possible. Average output power of 60 kW at 10.6 μm has been obtained from such a device.

Properties of the Gas-Laser Output Beam

Wavelength and Frequency. It is customary in laser terminology to refer to a laser transition by its wavelength (in micrometers or nanometers) and to discuss the fine structure of the transition in terms of frequency. Wavelength λ and frequency ν are related by $\lambda\nu = c$, where c is the velocity of light. The wavelength of a laser transition, as well as the wavelength interval or width of the transition over which optical gain exists, is a property of the laser atom or molecule. The transition width is also related to gas temperature and pressure. Typical widths of common gas lasers are:

Laser	λ, μm	Line width, MHz
HeNe	0.6328	1700
	1.15	920
	3.39	310
Ion laser	0.5	2500–3000
CO_2 low-pressure	10.6	60
High-pressure	10.6	800

Oscillation can occur at discrete frequencies (cavity modes) at frequency spacings of $\Delta\nu = c/2L$, where L is the separation of cavity mirrors. Depending on the nature of the laser medium and the geometry of the optical cavity, oscillation may occur at a number of different modes, within the line width of the transition. For example, for helium-neon at 0.6328 μm, with a cavity-mirror spacing of 100 cm, the mode spacing is 150 MHz, and 11 (axial) modes could oscillate. Single-axial-mode oscillation is generally achieved by reducing L so that only one axial mode lies within the line width of the laser transition. A stable optical cavity is required for both frequency and amplitude stability.

Available Gas Lasers

Of the many commercially available gas lasers (over 35 gas-laser species), four groups are most common: (1) low-power (few milliwatts) visible cw, including helium-neon (He-Ne) and helium-cadmium (He-Cd);

(2) medium-power (few watts), visible cw, including argon-ion (Ar^+) and krypton-ion (Kr^+); (3) medium- to high-power (10 to 10^4 W) infrared, cw, primarily carbon dioxide (CO_2) and ultraviolet wavelengths (rare gashalogen excimers, XeF, KrF, and so forth). These lasers along with a selected listing of other gas lasers are included in Table 9.2.5, which is arranged by wavelength, with cw and pulsed lasers listed separately. For many of the lasers, both the typical and the maximum available power or energy levels are given.

SEMICONDUCTOR LASER DIODES

Bart H. Verbeek

Introduction

Semiconductor laser diodes, or laser diodes in short, represent key components in the field of opto-electronics including optical communication, optical sensor technology, optical disc systems and material processing. They represent the smallest and most efficient of all lasers since it is based on the injection of carriers in a semiconductor *pn*-structure in combination with an optical cavity/resonator formed by the same semiconductor material. The *pn*-junction is operated in the forward direction and the injected carriers recombine at the *pn*-junction giving rise to the emission of photons. If the carrier density reaches a critical value, the light will be amplified and will yield in laser light emission. The injection current at which the laser start lasing is called the threshold current of the laser. The recombination of electrons and holes takes place in the active layer, sandwiched between a *p*-doped and *n*-doped cladding layer as shown in Fig. 9.2.10. These thin layers (= microns) are grown by epitaxial growth techniques on a semiconductor single crystal substrate with low defects. The dimensions of the laser chip are in the order of a few hundred micron (grain of salt size) but the active layer is much smaller (typically $1.5 \times 0.2 \times 250$ μm). Top and bottom of the laserchip are metallized to provide low ohmic contacts to the semiconductor material.

Since the laser diode is a small device and the aperture of the *optical beam* is in the order of the wavelength the light beam is divergent (Fraunhofer Diffraction). Semiconductor lasers require therefore a lens to couple the light from the chip into, e.g., an optical fiber or to generate a parallel beam. These lenses are usually provided in fiber-coupled packages together with a temperature stabilization unit (TEC). If the lens is not provided with the package (like TO-can type), external optics are required.

Laser diodes can be operated in the following modes:

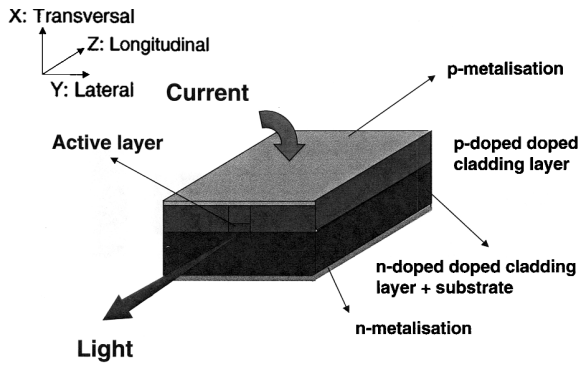

FIGURE 9.2.10 Schematic of semiconductor laser chip. The central area is the active layer surrounded by cladding layers. Top and bottom are metallized to provide electrical current injection. The laser light is a divergent beam because of diffraction emitted from the edge of the crystal. In the inset the definition of the transversal/lateral and longitudinal directions of the laser is given.

Continuous Wave (CW). A DC current flow will generate continuous emission of coherent light.

Amplitude Modulation. By modulation of the injection current, the optical output power can also be modulated. This is called direct modulation of the laser diode. Both analog as well as digital signals can be generated up to frequencies of 15 GHz.

Frequency Modulation. If a small ac injection current is applied to the dc current, the frequency of the emitted light is modulated (typically 100 MHz/mA), which can be employed in, e.g., FM transmission systems or suppressing Stimulated Brillouin Scattering in high-power optical transmission links.

Semiconductor lasers cover a wide spectrum in *emission wavelength* ranging from blue (450 nm) to be used in next-generation optical storage systems, via visible (red 633–650 nm), infrared (780–850 nm), IR (980 nm pump lasers), 1310, 1480, and 1520–1600 nm telecom wavelength) to FIR (>2000 nm for spectroscopy). Different semiconductor materials are used to achieve these wavelengths as will be discussed in the next sections.

Semiconductor Physics Background

Materials. In contrast to other lasers where the radiative transitions occur between atomic or molecular energy levels, semiconductor laser transitions occur between electronic bands, namely, the conduction band and valence bands of the semiconductor crystal. In particular, group III-V and II-VI compounds are *direct* semiconductors with efficient light-emitting characteristics (e.g., Si is an indirect semiconductor and does not radiate efficiently). Various III-V and II-VI materials are available; their ability to form solid solutions opened the possibility to vary the compositions in order to obtain the desired variations in bandgap and in refractive index, while maintaining lattice matching to the substrate. In Fig. 9.2.11 the solid dots represent the relationship between the bandgap E_g and the lattice constant of binary III-V compounds containing Al, Ga, or In and P, As, or Sb, and II-VI materials containing Cd or Zn and S, Se or Te, respectively. Since the photon energy E is approximately equal to the bandgap energy, the lasing wavelength λ can be obtained using $E_g = hc/\lambda$, where h is the Planck constant, and c is the speed of light in vacuum. If E_g is expressed in eV, the lasing wavelength in μm is given by $\lambda = 1.23889/E_g$.

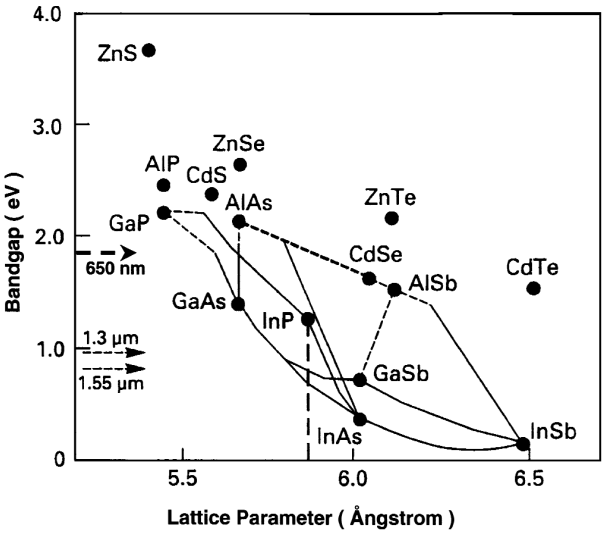

FIGURE 9.2.11 Graph showing the various semiconductor materials for making laser active and cladding layers. For each binary compound the lattice parameter and bandgap energy is given. Lines denote mixed compound solid solutions. As substrate material GaAs and InP are used for most lasers. Arrows indicate bandgap energy for three mostly used wavelength.

TABLE 9.2.6 Semiconductor Materials for Active/Cladding Layers and Their Wavelength Window/Applications

Substrate	Active/cladding layer	Wavelength range (μm)	Applications
GaAs	(Al)GaAs/AlGaAs	0.70–0.88	Optical disc
	(In)GaAs/AlGaAs	0.88–1.1	Pumping
	(In)GaAs/InGaP	0.88–1.1	High power
GaAs	(Al)GaInP/AlGaInP	0.60–0.67	Optical disc
	InGaAsP/AlGaInP	0.65–0.88	Laser printer
	InGaAsP/AlGaAs	0.65–0.88	Barcode/displays
InP	InGaAsP/InP	1.05–1.65	Fiber communication
	(Al)GaInAs/AlGaInAs		
Sapphire/SiC	InGaN/GaN	0.45	Optical disc
GaSb	GaInAsSb/AlGaAsSb	2–5	Spectroscopy laser radar

Figure 9.2.11 shows that the bandgaps and lattice parameters of $In_xGa_{1-x}As_yP_{1-y}$ (quaternary) compositions cover the area bound by connecting lines between the binaries InAs, InP, GaP, and GaAs, and can be grown lattice matched to InP and GaAs substrates for certain combinations of x and y. The interrelationships for the ternary $Al_xGa_{1-x}As$ follow the connecting line between the binary constituents GaAs and AlAs.

Lasers and other optoelectronic devices require a very low defect density in the crystal or else nonradiative processes will dominate over the radiative processes. Therefore, lattice matched crystal growth of the various compound layers on the substrate is essential and is achieved by modern epitaxial growth techniques such as MOVPE, MBE, and CBE. The semiconductor material can be doped with, eg., Zn (Si) to achieve p-type (n-type) doping. All modern semiconductor lasers consist of a double heterostructure in order to achieve high carrier densities at low currents by confining the recombining carriers in a small volume. The active layer is embedded between heterolayers having a larger bandgap—cladding layers. Wavelength ranges and applications for various substrates and active/cladding layers are given in Table 9.2.6. The pn-junction just occurs at the active layer, which has a lower bandgap. By injecting current in the diode, electrons from the n-side and holes from the p-side recombine in the active layer generating photons of the designed wavelength by the bandgap energy E_g (see Figs. 9.2.12*a* and 9.2.13). In order to reduce the total current, injection only takes place in a stripe of width w (typically 1–2 μm) (see also Fig. 9.2.10). The electrical diode characteristic of the laser is given by

$$I = I_0\left[e^{(e(V-IR_s)/nkT)} - 1\right] \tag{1}$$

where R_s is the series resistance of the diode and n is the ideality factor with $1 < n < 2$.

Now that carriers can recombine in the active layer, three processes will occur: (1) spontaneous emission, (2) stimulated emission, and (3) absorption of generated photons. At low injection current processes (1) and (3) dominate and the laser behaves as an LED. Only with sufficient carrier injection, the stimulated emission process will dominate and sufficient amplification of generated photons will occur. If the active layer is placed in an optical cavity preferred directional gain is obtained and laser action is possible. The optical material gain of the active layer is shown in Fig. 9.2.12*b* versus the wavelength, with increasing injection current as a parameter. With zero injection current, the material absorbs light for shorter wavelengths than λ_g, i.e., this material can be used as a photodetector. With increasing injection current gain is increasing and the maximum of the gain value shifts a little to lower wavelength because of bandfilling effects. For wavelengths beyond the bandgap energy (denoted as arrow) the material is transparant. The 3-dB bandwidth of the gain is typically 80 to 100 nm.

For efficient operation of the laser, the light that is generated in the active layer has to be guided within the laser structure. An optical waveguide is formed by the higher refractive index of the active layer with respect to the surrounding (cladding) layers. For stable laser operation it is required that this waveguide can only support the lowest-order mode (usually the TE_{00} mode) both in the transverse and lateral directions. Design parameters for obtaining a lowest-order mode are: thickness, width, and refractive index of the active layer and

the cladding layers. In Fig. 9.2.13 the transversal index profile and the resulting optical mode are shown. Several numerical tools are available to solve the Maxwell equations for the dielectric waveguide and obtain the optical mode profile in the laser (Near Field), external beam (Far Field), and astigmatism. Usually the optical mode (near Gaussian shape) is larger than the active layer and the fraction of light that travels in the active layer is called the *confinement factor* Γ (see Fig. 9.2.13).

With the gain medium in the active layer and the waveguide description to guide the light in the laser, the next step is the longitudinal *optical cavity*. Since the refractive index of the semiconductor lasers is about 3.3 to 3.4, which is much higher than air ($n \approx 1$), the simplest cavity is formed by cleaving the crystal to form the endfacet-mirrors. The (power) reflection is calculated as $R = [(n - 1)/(n + 1)]^2$ and results in about 30 percent. This value can be modified by applying appropriate dielectric facet coatings like AR or HR coating depending on application. A semiconductor laser based on cleaved facets is referred to as Fabry Perot lasers. Other cavity structures will be discussed later. A FP-cavity allows a set of discrete longitudinal modi which are determined by the condition that in a round-trip an integer number of wavelengths fit within the cavity of length, $n_e L$ where n_e is the effective refractive index. Allowed wavelengths are $\lambda_m = 2n_e L/m$, where m is the mode index. For evaluating the spacing between adjacent modi, $\Delta\lambda$, one must take into account the dispersion of the refractive index and the effective group index $n_{e,g}$ is introduced. The mode distance is given by $\Delta\lambda = \lambda^2/2n_{e,g}L$, which corresponds to the inverse round-trip delay τ_L of the cavity. With an effective group index of 3.5 and a laser cavity of 300 to 400 μm a typical round-trip delay is about 10 ps.

When the semiconductor active medium with gain profile, as shown in Fig. 9.2.12*b*, is placed in the Fabry Perot cavity to build a laser, this laser will start lasing at a wavelength corresponding to the mode with the highest gain. The spectrum of the FP laser consists then of a set of modi around this highest gain mode to form the spectrum of the FP laser.

Semiconductor Laser Parameters

The threshold for lasing in a Fabry Perot laser can be obtained by considering the intensity of the laserfield in a round-trip within the cavity. If the semiconductor material gain is denoted by G, the mode gain is given by $g = \Gamma G$ where Γ is the confinement factor and internal loss α_i the reflection coefficients R_1 and R_2 and length L, the net round-trip gain g_r is given by

$$g_r = R_1 R_2 e^{[2(g-\alpha_i)L]} \tag{2}$$

The material gain can be expressed in a linear relation to the current density N by $G = A(N - N_{tr})$, where A is the differential gain ($\partial G/\partial N$) and N_{tr} is the transparency current density, i.e., the value for injecting carriers such that the absorption and gain are equal and the material is transparent. At the lasing threshold, the optical field is sustained after traveling on round-trip in the cavity, thus the net round-trip gain g_r is unity, resulting in the threshold condition given by

$$g_{th} = \alpha_i + \frac{1}{2L}\ln\frac{1}{R_1 R_2} = \alpha_i + \alpha_m \tag{3}$$

where α_m is called the mirror loss.

The current density is related to the carrier density by

$$J = \frac{e d_{act} N}{\tau_n} \tag{4}$$

where d_{act} is the thickness of the active layer, and τ_n the carrier lifetime. The threshold current density J_{th} is now given by

$$J_{th} = \frac{J_{tr}}{\eta_i} + \frac{d_{act}}{\Gamma\beta\eta_i}\left(\alpha_i + \frac{1}{2L}\ln\frac{1}{R_1 R_2}\right) \tag{5}$$

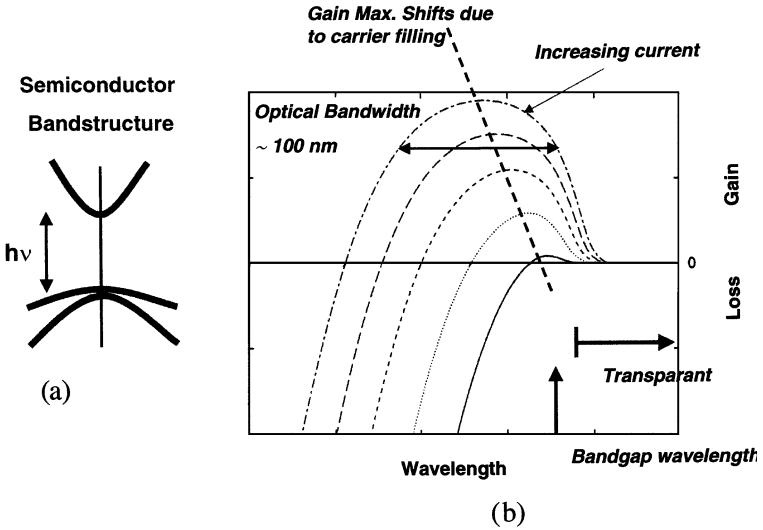

FIGURE 9.2.12 (a) Schematic representation of the conduction band and both valence bands of semiconductor laser crystals. The arrow denotes the bandgap energy determining the wavelength of the laser by $\lambda = 1.23889/E_g$. (b) Calculated gain spectrum of semiconductor materials as function of the wavelength. The vertical arrow indicates the bandgap wavelength, the horizontal arrow shows the transparent region of the material. The curves show the gain/absorption as a function of injection current density. Semiconductor lasers tend to operate near the gain maximum.

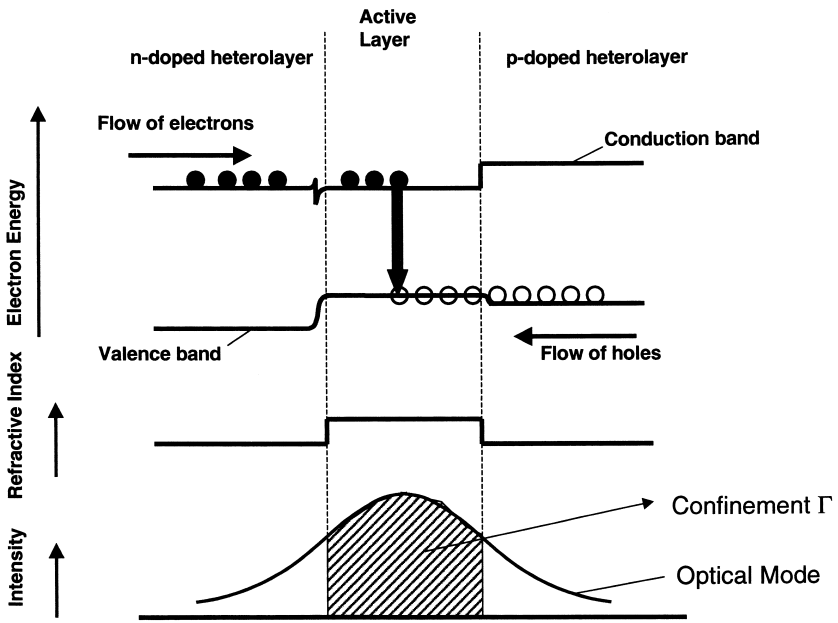

FIGURE 9.2.13 Top: Band diagram of a double heterostructure laser under forward current injection. Electrons (holes) flow from the n-(p-) doped cladding layer into the active layer with smaller bandgap giving radiative transitions emitting photons. Middle: Corresponding refractive index variation between cladding- and active region for waveguiding. Bottom: Optical intensity profile of the laser beam inside the laser cavity. The grey area is the part of the beam traveling in the active layer and defines the confinement factor Γ.

where J_{tr} is the current density to reach transparency, η_i is the internal efficiency with which electrons and holes recombine radiatively and β is the gain coefficient, which is related to the differential gain A by $\beta = A\tau_n/e$. Equation (5) shows that the threshold current consists of the transparency current density J_{tr} and a contribution to overcome the internal and mirror losses. By further increasing the injection current above threshold, the round-trip gain remains fixed, i.e., clamped to the value of g_{th} and the excess carriers are consumed to build up the laser oscillation intensity. The total optical power generated by stimulated emission in the cavity is given by

$$P = \eta_i \frac{h\nu}{e}(I - I_{th}) \tag{6}$$

where I and I_{th} are the driving and the threshold current, respectively, and $h\nu$ the photon energy. Part of this power is dissipated inside the laser cavity, and the remaining is coupled out through the facets. These two powers are proportional to the effective internal and mirror loss. The total output power from both facets is thus given by

$$P = \eta_i h\nu \frac{(I - I_{th})}{e} \frac{\alpha_m}{\alpha_i - \alpha_m} \tag{7}$$

The external differential efficiency is the ratio of the variation in photon output rate that results from an increase in the injection current and is given by

$$\eta_d = \frac{d(P/h\nu)}{d[(I - I_{th})/e]} = \eta_i \left[1 + \frac{2\alpha_i L}{\ln \frac{1}{R_1 R_2}}\right]^{-1} \tag{8}$$

In Fig. 9.2.14 the typical optical output power per facet (mW) versus the injection current (mA) (so called *L/I* curve) of a semiconductor laser is shown for various temperature where a photodetector is placed in front of the output facet of the laser. Up to the threshold current only spontaneous emission is generated but at threshold current the output power increases dramatically by the stimulated photons.

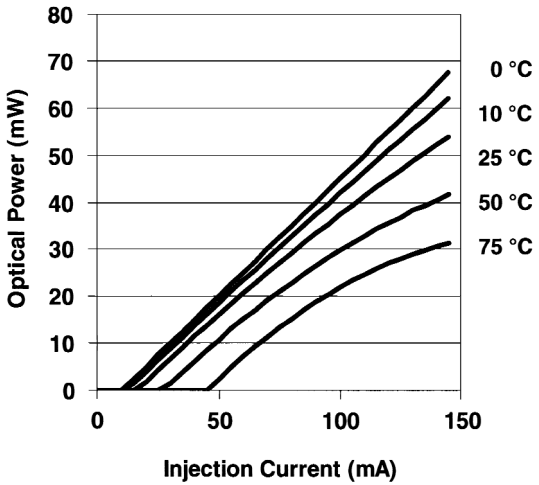

FIGURE 9.2.14 Light output power (mW) vs. injection current (mA)—L/I characteristic—of a semiconductor laser at various temperatures.

Several observations can be made from Fig. 9.2.14. First, the *L/I* curves are not exactly linear and deviate more at higher output power and high temperatures due to internal heating effects, increased internal losses and increased current (blocking) leakage. Second, the threshold current value increases with temperature owing to active layer temperature rise and additional loss mechanisms. The variation of the threshold current with temperature is expressed by an empirical relation:

$$I_{\text{th}}(T_2) = I_{\text{th}}(T_1)e^{(T_2-T_1)/T_0} \tag{9}$$

where T_0 is the characteristic temperature and T_1 and T_2 are expressed in Kelvin. T_0 values of 50 to 70 are found for InP-based lasers and >100 for GaAs-based lasers. It should be noted that T_0 is not constant over a wide temperature range.

The single-mode laser has a finite *linewidth* caused by spontaneous emission into the lasing mode adding phase noise. The well-known Shawlow-Townes expression for the linewidth of a semiconductor laser has been modified by Henry to include the dynamics of the carrier density on spontaneous emission events and the linewidth expression for a semiconductor laser is given by

$$\Delta v = \frac{h\nu v_g^2(\alpha_i + \alpha_m)\alpha_m n_{\text{sp}}}{8\pi P}(1+\alpha_H^2) \tag{10}$$

where $h\nu$ is the photon energy, n_{sp} is the spontaneous emission coefficient and α_H is Henry's parameter. This equation shows that increasing power, reducing internal and mirror losses and low α_H values result in narrow (Lorentzian) linewidth values. The linewidth of the laser is also related to the coherence length L_c that can be measured using a Mach-Zehnder interferometer to obtain the autocorrelation function via $L_c = c/\pi\Delta v$. Example: laser with linewidth of 10 MHz has a coherence length of about 10 m.

Optical Waveguiding

The photons generated by stimulated emission in the active layer must be guided in the semiconductor laser structure in order to optimize the gain (high confinement Γ). Guiding is also needed to generate a proper beam from the laser that can be coupled into a fiber with high efficiency or can be handled with bulk optical lenses. Beam profiles that have a Gaussian shape are preferred and these can be obtained when a dielectrical waveguide is designed to support the lowest order mode only. Two-dimensional waveguiding in the laser structure is formed by designing both the transversal direction (*x*, perpendicular to the active layer) and the lateral directional (*y*, in plane of active layer).

Transversal Guiding. This is determined by the refractive index difference between the active layer and the cladding layers (see also Fig. 9.2.13) and the thickness of the active layer. The parameter that determines the cutoff condition for higher-order modes is called the normalized frequency or simply the *V* parameter.

$$V = \frac{\pi d}{\lambda}\sqrt{n_{\text{act}}^2 - n_{\text{cladding}}^2} \tag{11}$$

where *d* is the thickness of the active layer. In order to obtain single mode operation, the *V* parameter should obey $V < 2.4$, which is easily met with thin active layers and optimized cladding layers for carrier confinement.

Lateral Guiding. It is less straightforward mainly because of technological constraints. Three classes of lateral guided laser structures can be distinguished (Fig. 9.2.15).

1. *Gain guided structure.* A continuous active layer with no lateral index variation. Current injection in a stripe top contact results in local gain under the stripe and optical losses away from the stripe, hence the name gain guiding. The laser beam shows considerable astigmatism and a non-Gaussian lateral profile at high-power levels. It is used in very high-power lasers with a wide stripe where the beam properties are less

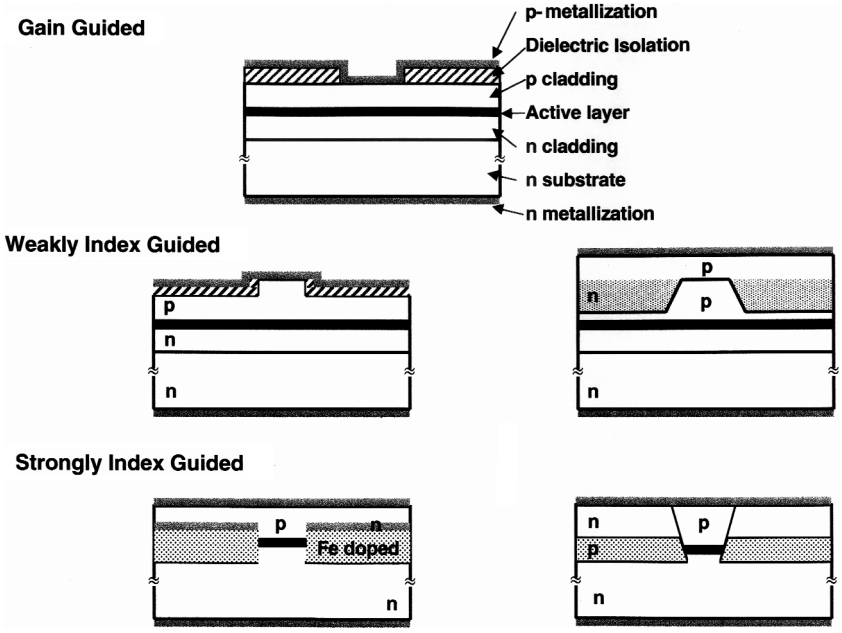

FIGURE 9.2.15 Lateral laser structures for lateral optical guiding. Top: Gain guided laser, Center: Weakly index guided structures (Ridge waveguide and buried Ridge structure). Bottom: Strongly index guided laser structures (SI-PBH, semi-insulating planar buried hetrostructure and *n-p-n* blocking structure).

important. Many lateral higher-order modes are present but this can be reduced by employing a longitudinal taper structure in the stripe.

2. *Weakly guided structure.* A continuous active layer but with a lateral index variation in the top/bottom cladding layer by processing, e.g., ridge structure or buried ridge structure. The lateral index guiding is small (^{a}10-3) compared to the transversal confinement giving rise to elliptical beam profile.
3. *Strongly index guided structure.* The active layer is surrounded by cladding type material giving rise to both lateral and transversal strong index contrast and waveguiding with almost circular beam profiles. Strongly index guided laser structures are fabricated using several epitaxial growth and regrowth and processing steps. These structures have efficient current injection in the active layer of typically 1.5 to 2 mm width.

Longitudinal Laser Structures

Fabry-Perot Laser. The simplest longitudinal structure laser is a chip that is cleaved to form facets with reflectivity R to achieve optical feedback. These facets can be coated to modify the reflection value from low (AR) to high (HR). This structure allows for a discrete set of cavity modes and in combination with the gain profile, which is parabolic in shape, the laser operates in a series of modes around the gain maximum. The associated spectrum is called multilongitudinal mode and is depicted in Fig. 9.2.16. The number of modes (5 to 30) depends on the output power of the laser and decreases with increasing power. These modes operate simultaneously as is proven by the occurrence of frequency doubled components in the spectrum.

DFB Laser. In fiber optic long distance applications the multimode emission spectrum in FP lasers restricts the transmission distance because of the material dispersion of the fiber. To improve the link distance the need

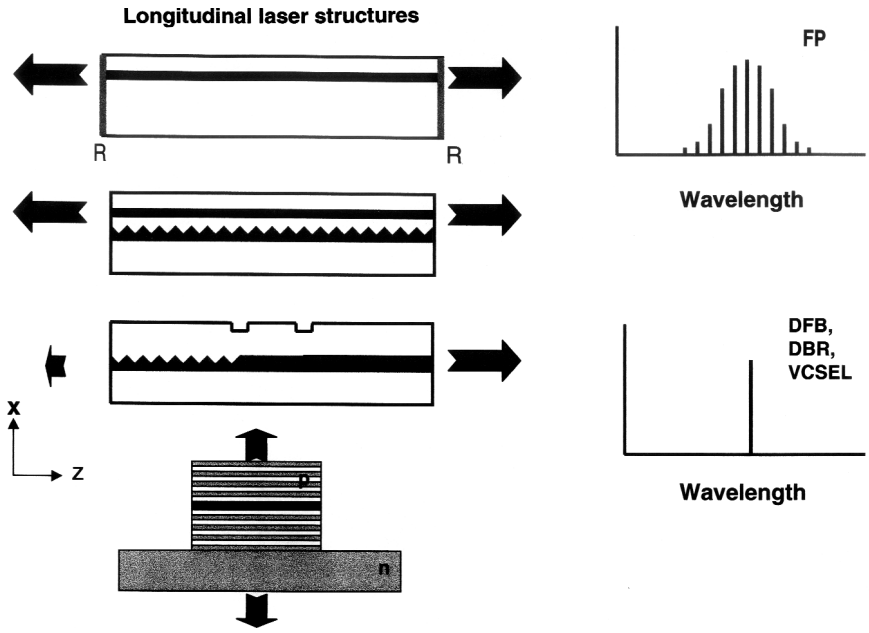

FIGURE 9.2.16 Longitudinal laser structures and corresponding spectral behavior. From top to bottom: Fabry Perot laser, DFB (distributed Bragg reflector) laser, DBR (distributed Bragg reflector) laser, and VCSEL (vertical cavity surface emitting laser).

for a narrow spectral width laser has led to the development of the distributed feedback (DFB) laser emitting a narrow (few MHz) single longitudinal mode. The DFB laser is characterized by a grating near (above or below) the active layer in the longitudinal structure. The analysis of the coupled modes in the DFB laser is too lengthy to be discussed here and can be found in the reference books. The lasing wavelength of the DFB laser is to first approximation determined by the grating pitch Λ and the effective refractive indiex of the waveguide and is given by $\lambda = 2n_{\text{eff}}\ \Lambda$. Using $\lambda = 1550$ nm and $n_{\text{eff}} = 3.25$ this results in a submicron grating pitch of 0.2384 μm. This grating requires an additional transparent guiding layer in which the grating is made using holographic exposure or e-beam pattern generator. The accuracy of the laser wavelength needed in DWDM systems (e.g., 50 GHz spacing) requires a controlled grating pitch fabrication within 30 pm! Since DFB lasers have an internal feedback for laser operation, the facets need to be eliminated by applying AR coatings on both sides. The position of the laser wavelength with respect to the gain maximum is a design parameter and usually the negative detuning of 10 to 30 nm (i.e., laser wavelength is positioned on the short wavelength side of the gain peak) is applied for improved modulation properties. The spontaneous emission spectrum of DFB lasers (i.e., subthreshold) is characterized by a so-called stopband. The width of the stopband is linearly related to the coupling coefficient parameter κ of the grating to the optical mode. Standard DFB lasers have a nonuniform power distribution in the longitudinal cavity, which can be modified/improved by including phase shifts in the grating. Single $\lambda/4$-phase shift but also multiple $\lambda/8$ or $\lambda/16$ have been introduced to improve the uniform power density that is required for linear *L/I* characteristics in, e.g., analog transmission. The linewidth of DFB lasers is sub-MHz.

DBR Laser. In a distributed Bragg reflector (DBR) laser one of the facets is replaced by a waveguide structure with grating, which serves as a wavelength selective reflector. In contrast to the DFB laser, the active layer (= gain region) is now separated from the wavelength selection element (Bragg section). This Bragg section consists of a transparent guiding layer with an etched grating and cladding layers. This section is "butt-coupled" to the active section where the active layer provides the waveguiding. In many DBR lasers, an

intermediate section is applied in order to be able to provide round-trip phase matching for the lasing mode. The DBR wavelength is determined by the overlap of one of the cavity modes and mode with highest reflectivity. Since the reflector is positioned at the rear of the laser structure, most power is emitted from the front facet. From a technology point of view, this structure is more complex and requires more regrowth steps than the DFB laser. This structure is also very suited to make wavelength tunable lasers. The optical spectrum shows single frequency with MHz linewidth.

VCSEL. In a vertical cavity surface emitting lasers (VCSELs) the active layer is sandwiched between two highly reflective DBR mirrors (>90 percent) epitaxially grown on the substrate. The first VCSELs were made on GaAs substrate with many pairs of AlAs and GaAs as multistack reflectors operating at wavelength of 850 and 980 nm. Also InP-based VCSEL are available for the 1310 to 1550 nm telecom applications. The laser operates in a single longitudinal mode by virtue of an extremely small cavity length (about 1 μm) for which the mode spacing exceeds the gain bandwidth. Light is emitted in a direction normal to the active layer plane and since the output power has to pass the high reflector, VCSELs are characterized by low output power levels (few mWs). An important advantage of the VCSELs is the beam shape, which can easily be made narrow and symmetrical which allows direct fiber coupling without additional optics. This, along with the possibility of on-wafer testing, is viewed as considerable cost saving. Direct modulation has been achieved up to 2.5 Gb/s. Application areas are optical interconnect and short haul optical data links.

Dynamic Properties of Semiconductor Lasers

Rate Equations. One of the virtues of semiconductor laser diodes is their capability to modulate the optical output power directly with the injection current. To analyze the modulation aspects it is necessary to consider the laser diode dynamics on the basis of the single mode rate equations for the photon density S in the optical mode and the carrier density N in the active medium. These equations can be written as

$$\frac{dS}{dt} = \Gamma v_g g(N,S)S - \frac{S}{\tau_p} + \Gamma\beta\frac{N}{\tau_n} \tag{12}$$

$$\frac{dN}{dt} = \frac{I(t)}{eV_{\text{act}}} - \frac{N}{\tau_n} - v_g g(N,S)S \tag{13}$$

Here v_g is the group velocity, Γ is the optical confinement factor, V_{act} is the volume of the active medium, e is the electronic charge, $I(t)$ is the (modulated) pump current, τ_p is the photon lifetime, τ_n is the carrier lifetime, and β is the fraction of the spontaneous emission that couples into the lasing mode. The first equation represents the photon density variation owing to the photon generation by stimulated and spontaneous emission and the photon loss at the mirrors and by absorption. The second equation describes the carrier density variation resulting from the carrier injection by the pump current $I(t)$ and the carrier annihilation by the stimulated and spontaneous recombination. The material gain $g(N,S)$ (per unit length) depends on both the carrier density and the photon density and is modeled as

$$g(N,S) = \frac{\partial g}{\partial N}(N - N_{\text{tr}})(1 - \epsilon S) \tag{14}$$

Here the gain is linearized at the transparency carrier density N_{tr} with a gain slope constant $\partial g/\partial N$ (differential gain) and the gain dependency on the photon density S is characterized by the gain suppression parameter ϵ.

The rate equations cannot be solved analytically; however, the small signal response of a laser diode can be derived by linearizing the rate equations and applying a small signal analysis. Then the intensity modulation transfer function normalized to the zero frequency response $M(0)$ is given by

$$\left|\frac{M(j\omega)}{M(0)}\right| = \frac{\omega_0^4}{(\omega^2 - \omega_0^2)^2 + \gamma^2\omega^2} \tag{15}$$

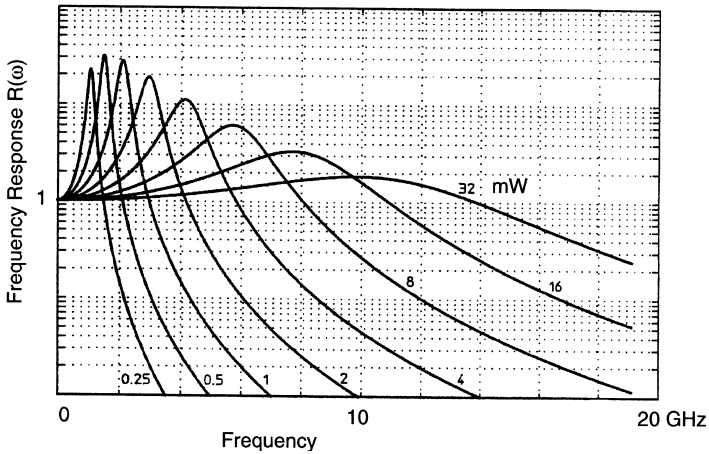

FIGURE 9.2.17 Calculated small signal laser diode response as function of the output power from 0.25 to 32 mW.

with the circular relaxation oscillation (RO) frequency given as

$$\omega_0^2 = \frac{v_g}{\tau_p}\frac{\partial g}{\partial N}S \tag{16}$$

and the damping factor γ

$$\gamma = \frac{\beta\Gamma N}{S\tau_n} + \frac{1}{\tau_n} + v_g\frac{\partial g}{\partial N}S + \frac{\epsilon S}{\tau_p} \tag{17}$$

As an example the calculated small signal response for a semiconductor laser diode at several output powers is given in Fig. 9.2.17. The intrinsic frequency response of a laser diode is completely described and shows a second-order low pass network nature. The transfer function is characterized by a clear resonance followed by a steep roll-off. The resonanace known as the relaxation oscillation results from the interplay between the photon field and the carriers. The resonance frequency ω_0, obtained from the small signal analysis, increases with the square root of the optical power. The damping of the resonance is determined by the spontaneous emission at low photon densities and by the gain suppression factor ϵ at high photon densities. In view of high frequency modulation an ultimate increase of the relaxation oscillation frequency is desired but will be severely limited at high photon densities by the damping introduced by the gain suppression ϵ.

In addition to the maximum intrinsic modulation frequency, parasitic capacitance in the laser structure and/or mounting are also determining the small signal response of laser diodes. To account for the chip and bonding parasitic capacitance, it should be expanded as

$$R(\omega) \approx \frac{\omega_0^4}{(\omega^2 - \omega_0^2)^2 + \gamma^2\omega^2}\frac{1}{1 + \omega^2(RC)^2} \tag{18}$$

In digital modulation schemes the large signal nonlinear modulation response should be taken into account and the small signal approach is not sufficient. A typical response on a rectangular current pulse is schematically given in Fig. 9.2.18. Important parameters here are the turn-on and the turn-off time. Moreover, frequency ringing will occur when the laser diode is switched from the "off" state to the "on" state (and back)

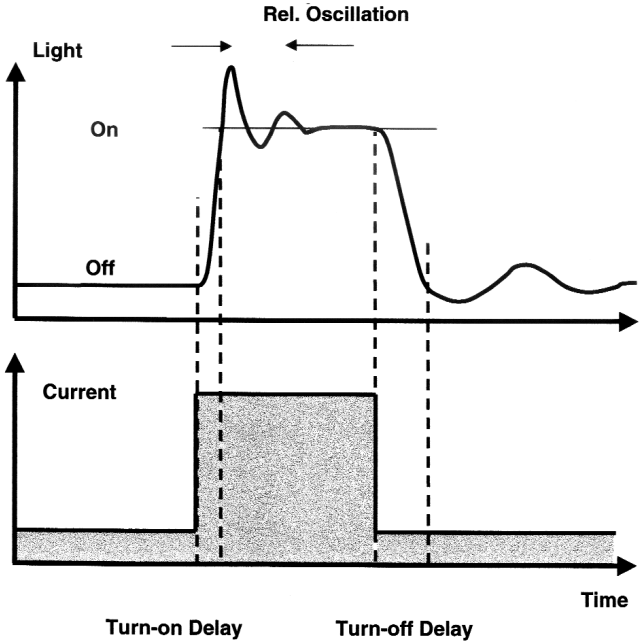

FIGURE 9.2.18 Large signal optical modulation response of a laser diode on rectangular current pulse.

with correspondingly different relaxation oscillation frequencies and damping factors. The turn-on time t_{on} for $I_{off} > I_{thr}$ can be calculated as

$$t_{on} = \frac{0.23}{f_0}\sqrt{\ln\left(\frac{S_{on}}{S_{off}}\right)} \tag{19}$$

with $f_0 = \omega_0/2\pi$ is the relaxation oscillation frequency corresponding to the "on" state, S_{on} is the steady-state photon density in the "on" state, and S_{off} in the "off" state. Considering a high-speed laser diode with $f_0 = 10$ GHz and an extinction ratio of 6:1 yields a turn-on time t_{on} of 31 ps. The turn-off time t_{off} can be approximated as $(0.5–2)t_{on}$. As the relaxation oscillation frequency corresponding to the "off" state with $S_{off} << S_{on}$ is several factors lower than f_0, the turn-off time is larger than the turn-on time.

A powerful tool to predict the performance of laser diodes is given by simulation. By numerical integration of the rate equations the time domain response of the laser output power can be calculated when a time-varying input current $I(t)$ is inserted. The results of simulations are represented as eye patterns (Fig. 9.2.19) obtained with a 10 Gb/s2^7–1 PRBS data formats. The laser extinction ratio is approximately 6:1.

Optical Frequency Response of Laserdiodes. When a modulated current is injected into a laserdiode, the varying carrier density will affect the refractive index of the active medium because of carrier-induced band-edge shifting. This implies that not only the photon density S will be modulated by the gain variations, but also the lasing resonance frequency by the varying refractive index. This optical frequency response (in intensity modulated direct detection systems regarded as highly undesirable) is denoted as *frequency chirp*. The so-called linewidth enhancement or Henry's factor α_H describes this coupling between the gain and the refractive index and is given by

$$\alpha_H = -\frac{4\pi}{\lambda}\frac{(\partial n_{eff}/\partial N)}{\Gamma(\partial g/\partial N)} \tag{20}$$

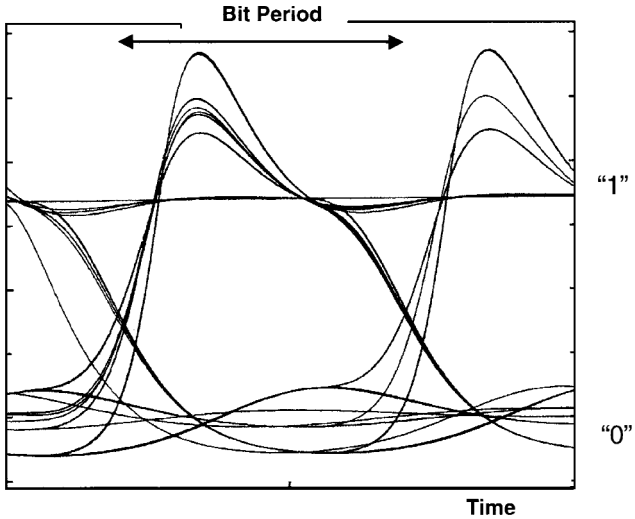

FIGURE 9.2.19 Simulated 10 Gb/s eye patterns (I_{off} = 18 mA, I_{on} = 54 mA) for SL-MQW active layer laser diode.

With this α_H parameter the expression for the frequency variation under injection current modulation is expressed as follows:

$$\Delta\nu(t) \cong \frac{\alpha_H}{4\pi}\left[\frac{1}{P(t)}\frac{dP(t)}{dt} + \frac{2\Gamma}{h\nu\eta_d V_{act}}\epsilon P(t)\right] \tag{21}$$

where η_d is the differential efficiency. In this equation, two chirp contributions are present. The first part (*transient chirp*) is associated with the transients and the ringing introduced by the relaxation oscillation when the laser is switched between the "on" and the "off" states. The second contribution is governed by nonlinear gain suppression coefficient ϵ and originates from the imperfect carrier density pinning because of the nonlinear gain. This *adiabatic chirp* depends on the laser structure and causes a frequency offset during modulation between the "on" state and the "off" state. The total chirp is directly proportional to the α_H-factor that highlights the significance of this parameter. Typical α_H-factors range from 2 to 6 depending on the detailed structure of the active layer and laser structure.

The laser frequency variations as function of the time can be calculated by numerical integration of the rate equations. Figure 9.2.20 shows the optical output power (dashed curve) and the corresponding frequency response (solid curve) for a single 2.5 Gb/s pulse (400 ps). The zero chirp value is related to the CW "on" state.

The optical frequency response of laser diodes poses severe problems in intensity modulated direct detection systems employing dispersive fibers. The addition of spectral components by chirp increases the total frequency bandwidth. In combination with fibers showing a substantial dispersion at the operating wavelength (–17 ps/nm/km) (@ 1550 nm), the frequencies that compose the signal travel with a different group velocity along the fiber. This results in a frequency dependent arrival time of the signal components and hence signal distortion at the receiver side. In digital systems information associated with one bit can occur in a neighbor bitslot giving rise to intersymbol interference (ISI).

Active Layer Structures

Quantum Well Lasers. The development of advanced crystal growth techniques like metallo-organic chemical vapor phase epitaxy (MOVPE) and molecular beam epitaxy (MBE) allowed the growth of defect-free

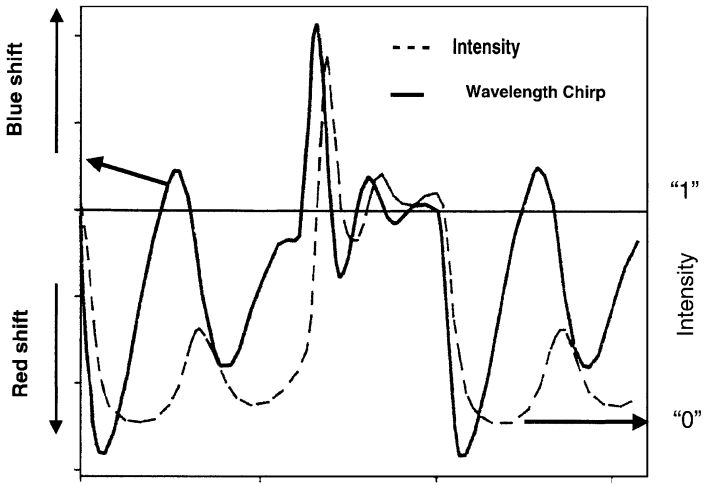

FIGURE 9.2.20 Simulation of the frequency response (solid curve) and the large signal response (dashed curve) of a bulk laser diode.

ultrathin layers with sharply defined heterointerfaces. The creation of these layers with a thickness close to the Broglie wavelength of electrons accelerated the development of single quantum well (SQW) and multiquantum well (MQW) laser diodes. For conventional bulk laser diodes the active layer thickness is about 150 nm or more. The active layer of quantum well lasers consists of one or more thin layers ($L_z < 30$ nm) which are separated by barrier layers with a larger bandgap material. For injected carriers confined to these wells, the energy for motion normal to the well is quantized into discrete energy levels. The motion of electrons/holes in the plane of the quantum well is not quantized and form continuous states. The heterostructure for bulk active layer, as shown in Fig. 9.2.13, is now modified as shown in Fig. 9.2.21. Here the conduction and valence band structure is shown for a MQW laser having four quantum wells. For every quantum number, one conduction band and two valence band (namely, the heavy and light holes) levels exist. These levels are degenerated. In the z direction the carriers are confined in the well as a particle in a box of width L_z and the calculation of the

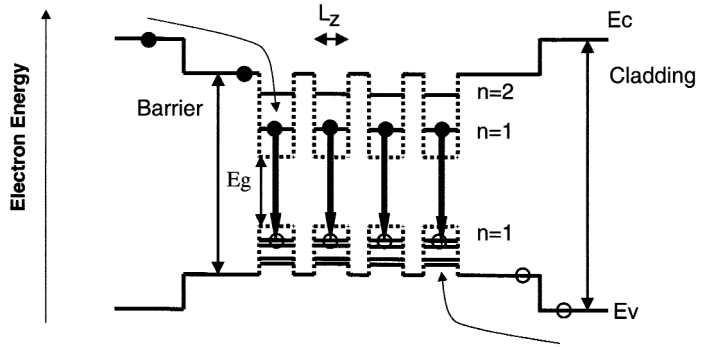

FIGURE 9.2.21 Schematic band energy diagram of a four quantum well active layer showing the conduction and valence band. The well width is L_z. The dashed lines indicate the energy corresponding to the material composition and the solid lines show the energy levels for ($n = 1,0, \ldots$) because of the quantum effect ("particle in box"). Arrows show the radiative transitions between electrons (filled balls) and holes (open balls).

allowed energy states is a well-known quantum mechanical problem. The energy levels associated with this "particle-in-box" is given by

$$E_n = \frac{h^2 n^2}{8mL_z^2} \tag{22}$$

which is valid for both electrons and holes. Here n is the quantum number, L_z is the quantum well width (QW layer thickness), m is the effective mass for this level, and h is Planck's constant. The effective bandgap of quantum wells is given by $E_g = E_g^{\text{bulk}} + E^c_{n=1} + E^c_{n=1}$, and thus is a function of the well thickness L_z; i.e., by using the same composition in the QW, the emission wavelength can be adjusted by changing the well width. Furthermore, the gain spectrum and the gain current relations lead to improvements for laser operation such as a reduction of the threshold current and its temperature sensitivity, enhancement of the differential quantum efficiency, an increase in modulation bandwidth and a reduction of the spectral linewidth (lower α_H). These improvements have been observed mainly in AlGaAs-based lasers and to a lesser extent in InP-based lasers because of higher intervalence band absorption processes.

Strained Quantum Well Lasers. To further improve the transition efficiency of MQW lasers, in particular for InP-based lasers, mechanical strain in the QWs can be introduced by growing lattice mismatched epitaxial layers on a thick substrate. These layers are subjected to a biaxial in-plane strain. As an example, the growth of $In_xGa_{1-x}As$ with $x = 0.53$ is lattice-matched to InP substrate. For $x > 0.53$, i.e., large In atom rich, the lattice is compressed in the x-y plane and is called compressive strain. For $x < 0.53$, i.e., smaller Ga atom rich, the strain is tensile. The lattice mismatch is bound by the critical thickness limitation depending on materials (elastic constants), degree of lattice mismatch and substrate orientation, and sets an upper limit to the applied strain before lattice defects such as misfit dislocations occur. Because of the deformation of the unit cell of the crystal, the bandstructure of the semiconductor material is modified. For InGaAs/InP materials the effect is most pronounced in the valence subbands, namely, the removal of the valence subband degeneracy and a larger split of the valence bands. This results in more efficient electron-hole transitions and reduction of the intervalence band absorption leading to much improved laser performance such as threshold current reduction, higher differential gain, lower α_H parameter, less temperature sensitivity, and TE or TM emission control.

Quantum Dot Lasers. Quantum dot (QD) or quantum dash-lasers are characterized by an active layer consisting of small clusters of active material embedded in cladding material. These clusters are made of InAs using the self-assembly property in crystal growth using MBE or MOVPE. Self-assembled QDs form spontaneously on the GaAs surface during growth because of lattice mismatch between InAs and GaAs. The InAs islands are then capped by another GaAs layer. Since the GaAs conduction (valence) band minimum (maximum) has higher (lower) energy than that of InAs, both electrons and holes are trapped by the InAs island (QDs). The shape of these QDs depends on the growth conditions. Typically, the size is strongly asymmetric: the in-plane diameter of the QDs ranges from 20 to 40 nm, whereas the height ranges from 2 to 6 nm. Nevertheless, the electrons and holes are now trapped in three dimensions unlike the quantum well (one-dimensional) or the quantum wire (two-dimensional) giving rise to new physical properties when applied in an optical cavity. The transitions within the QD are now uncoupled from the surrounding QDs modifying the gain dynamics. Also, QD-lasers have been fabricated to obtain 1300-nm-emitting lasers using GaAs as substrate and allowing much higher T_0 values than for InP-based lasers.

Quantum Cascade Lasers. The principle of quantum cascade laser is based on quantum confinement in quantum wells (with associated energy levels) and the tunneling property of electrons through energy barriers. In contrast to usual semiconductor lasers where the emission process is based on transitions between conduction band and valence band, in QCLs the transitions take place between the higher energy state of one QW and a lower energy state of the nearest neighbor QW as schematically depicted in Fig. 9.2.22. By applying many QWs in the active layer with carefully designed barriers, a single electron is able to generate more than one photon, thus allowing high power operation. The wide wavelength range in FIR (3 to 30 μm) can be obtained by properly designed QW and barrier layer thickness. The efficient photon generation allows high output power levels in the watt range. These QCLs are applied in environmental sensing and polluting monitoring, process control, automotive, and medical analysis.

Other Semiconductor Lasers

Analog Lasers. Semiconductor lasers are used as the optical source in fiber optic cable television systems where a large number (up to 200) channels—having independent frequencies in the range between 25 and 301 MHz or even to 860 MHz—are multiplexed on the optical carrier and broadcasted. This amplitude-modulated subcarrier lightwave CATV system requires extremely linear transfer characteristic of the laser, i.e., a linear *L-I* curve. If not, intermodulation products result from the modulation of the laser current with the frequency channels. If these intermodulation products have frequencies corresponding to one or more of the TV channel frequencies, distortion of the signals arises. A measure of the distortion is the so-called CSO (composite second order which is the sum of all mix frequencies by f_m and f_k at $|f_m \pm f_k|$) and CTB (composite triple beat; $|f_m \pm f_k \pm f_1|$). CATV lasers are specified by IM2 < –45 dBc and IM3 < –50 dBc. Also low noise in the optical power is important. The relative intensity noise (RIN) should be below –155 dB/Hz in a frequency interval between 100 kHz and 2.5 GHz. CATV lasers are characterized by high optical output power (>20 mW) allowing a higher split ratio in the broadcast mode.

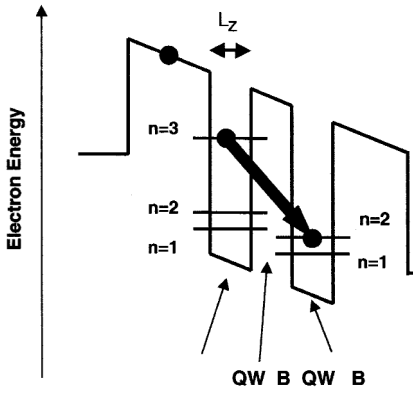

FIGURE 9.2.22 Schematic conduction band energy diagram of a quantum cascade laser with three QWs of width L_z. In the left well the energy levels corresponding to $n = 1$, 2, and 3 is indicated by the horizontal lines. Tunneling of the electron takes place through the intermediate barrier B and an electron transition between $n = 3$ state to the $n = 2$ state of the nearest QW is shown by the arrow.

Tunable Lasers. Semiconductor tunable lasers have the property that the emission wavelength can be tuned by thermal/mechanical/electronic means. This feature makes tunable lasers very attractive in DWDM applications in fiber optical systems, fiber sensor applications, environmental sensing, and instrumentation. A vast variety of technical solutions have been proposed and introduced in the market that offer wavelength tunability and maintaining the prime characteristics of nontunable lasers such as the DFB laser, i.e., high power, low noise, spectral purity, and small footprint. Also the tuning speed is an important differentiator and ranges between several ns for semiconductor solutions to ms to mechanical and thermal solutions. A good overview of all tunable laser concepts can be found in the textbook of Amann and Buus (1998) on this topic. Tunable semiconductor lasers can be classified into four groups:

Temperature tunable lasers (TTLs). The wavelength of the diode laser increases with temperature because the material gain is temperature dependent with $d\lambda/dT = 0.5$ nm/K. For DFB lasers with an internal grating the wavelength tunability is much less because only the temperature dependence of the effective mode index has to be taken into account. The $d\lambda/dT$ for DFB lasers is 0.08 nm/K. Using the internal TEC in the laser package, the wavelength can be tuned thermally over typically 3.5 nm.

External cavity lasers (ECL). This concept uses a FP laser chip of which one of the mirrors is AR-coated and the light from this facet is reflected back by an external grating that can rotate. The grating gives wavelength selective feedback and the achievable tuning range is usually determined by the gain bandwidth of the active layer of the FP laser. A tuning range of 100 nm can easily be obtained. The front mirror and the grating form the laser cavity, which is usually long (centimeters) so many "external cavity modes" are present. Laser linewidth is excellent (<100 kHz). This laser is mainly used in instrumentation applications. Recent developments in microelectromechanical systems (MEMS) have revealed miniature ECLs using a grating. An alternative to the grating is a set of etalons between the AR-coated facet and a retroreflector. If one of the etalons is made variable, then a differential etalon external cavity is obtained.

Multisection lasers. Here the laser chip is split up into a number of electrically separated longitudinal segments where independent injection currents can be applied. The physical mechanism for tuning the wavelength is the free-carrier effect. The refractive index change Δn caused by injection of carriers is proportional to the carrier density, which in turn has a nonlinear relationship with the tuning current resulting from Auger recombination processes. The maximum achievable Δn is about –0.04, whereas the thermally induced index change is in the order of +0.01. Examples of multisection lasers based on tuning current injection only

are 2-section DFB, 2- and 3-section DBR laser and tunable twin guide lasers. Maximum achievable tuning range is determined by $\Delta\lambda/\lambda \approx \Delta n/n$ and is typically 15 nm. For increased tuning ranges, so-called *widely tunable lasers*, use is made of the Vernier effect in sampled grating DBR lasers having a comb-like reflection spectrum from sampled gratings in two sections. The sampled grating consists of several sections of interrupted grating. The SG-DBR has four sections with the active and phase control section in between two sampled Bragg reflectors with slightly shifted periods. Tuning range of 50 nm can be achieved with this laser although with moderate output power because the beam has to propagate the SG reflector. Another structure is the superstructure grating DBR using a chirped grating giving more uniform reflection peaks. Tunable multisection lasers using codirectionally coupled waveguides provide an additional internal mode filter to discriminate between cavity modes. An example of this structure is the grating-assisted codirectional coupler with rear sampled grating reflector (GCSR) laser. This laser achieves over 100 nm tuning range. Multisection tunable lasers require sophisticated control loops to adjust the individual wavelengths and is usually delivered with the device.

Vertical cavity lasers. If the top mirror of a VCSEL is made movable by applying MEMS technology, the single longitudinal mode that can exist in the small cavity can be tuned in wavelength. Up to 50 nm tuning range can be achieved with a simple control algoritm. However, the output power is low as a consequence of the VCSEL structure.

Pump Lasers. Semiconductor lasers that can deliver high ouput power into the optical fiber for erbium-doped fiber amplifiers (EDFAs) and RAMAN amplifiers (for C- and L-band) are called pumplasers. Amplifier designs developed before 2001 incorporate the 14xx (1405 to 1520 nm), 1480 and 980 nm pump lasers with power levels of typically less than 200 mW. The 980-nm-based pumplasers are fabricated using InGaAs/AlGaAs/GaAs materials with a wide spot size to reduce catastrophic optical mirror damage because of facet erosion due to the high optical flux. Ridge waveguide (weakly index guided) laser structures are the common laser design. The other pump sources are based on InGaAs/InP material system where COD is no issue and an optimum fibre chip coupling can be achieved by beam design. Index-guided laser structures are used here. Pump lasers for the next generation of optical networks will typically have more than 300 mW of power. In order to increase the power level, hybrid integration of pump modules by, e.g., polarization multiplexing, allow for power levels up to 1 W.

Optical Storage Lasers. Historically, the first optical disc lasers were made in GaAs/AlGaAs lasers operating at a wavelength of 820 nm. Since the spot size on the disc to read and/or write data is proportional to $\lambda/2\text{NA}$ where NA is the numerical aperture of the lens, a higher optical capacity can be obtained by developing semiconductor lasers operating at shorter wavelengths. This has led to weakly guided 780 nm GaAs/AlGaAs-lasers for the CD application and 633 nm lasers based on AlInGaP/InGaP/GaAs materials for DVD. To further increase the density, green lasers have been investigated based on II-VI materials using ZnSe/ZnSSe/GaAs materials but these lasers suffered from reliability problems because of crystal defects. Recent developments of InGaN/GaAlN/GaN on sapphire substrate-based lasers, emitting in blue 450 nm, have led to a capacity of 15 Gbyte of digital data on a single layer. Also based on InGaN materials, semiconductor lasers emitting 405 nm, i.e., blue-violet color have been made for optical data-storage systems such as DVD and future systems.

BIBLIOGRAPHY

Lasers

Cheo, P. K., "Far-infrared lasers for power cable manufacturing," *IEEE Circuits and Devices Magazine*, January 1986.

Dixon, J. A., "Laser Surgery and the Physical Sciences," 1986 Conf. Lasers and Optics.

Dye Lasers Conference Session, 1985 Conf. Lasers and Electro-Optics.

Gill, T. E., AVLIS Laser Data Acquisition and Control System, 1986 Southeastern Symp. System Theory.

Industrial Laser Review Buyers' Guide to Companies and Products Issue, Pennwell, July 1995.

Kujawski, A., and M. Lewenstein (eds.), "Quantum Optics," *Proc. Sixth Int. School of Coherent Optics*, Reidel, 1986.

Laser Focus World Buyers' Guide, Pennwell, 1995.

Laser Focus World Medical Laser Buyers' Guide, Pennwell, 1995.

Rhodes, C. K. (ed.), "Topics in Applied Physics," Vol. 30, Excimer Lasers, 2nd ed., Springer-Verlag, 1984.

Voyles, R. M., "Non-contrast Bent Pin Detection Using Laser Diffraction," 1986 Electronic Components Conference.

Young, M., "Optics and Lasers: Including Fibers and Integrated Topics," Springer, 1984.

Semiconductor Lasers

Agrawal, G. P., and N. K. Dutta, "Long Wavelength Semiconductor Lasers," Van Nostrand Reinhold Company, 1986.

Agrawal, G. P., "Fiber Optic Communication Systems," Wiley, 1997.

Amann, M. C., and J. Buus, "Tunable Laser Diodes," Artech House, 1998.

Botez, D., "Laser diodes are power packed," *IEEE Spectrum*, June 1985.

Chang, K. (ed)., "Handbook of Microwave and Optical Components," Vol. 3, Optical Components, Wiley Interscience, 1990.

Cheo, P. K. (ed.), "Handbook of Solid-State Lasers," Marcel Dekker, 1989.

Gillessen, K., and W. Schairer, "Light Emitting Diodes: An Introduction," Prentice Hall, 1987.

Hecht, J., "The Laser Guidebook," 2nd ed., McGraw-Hill, 1992.

"Laser Diode Operator's Manual and Technical Notes," SDL, 1994.

Peterman, K., "Laser Diode Modulation and Noise," Kluwer Academic Publishers, 1991.

Zeman, J., "Visible diode lasers show performance advantages," *Laser Focus World*, August 1989.

Zory, P. S., "Quantum Well Lasers," Academic Press, 1993.